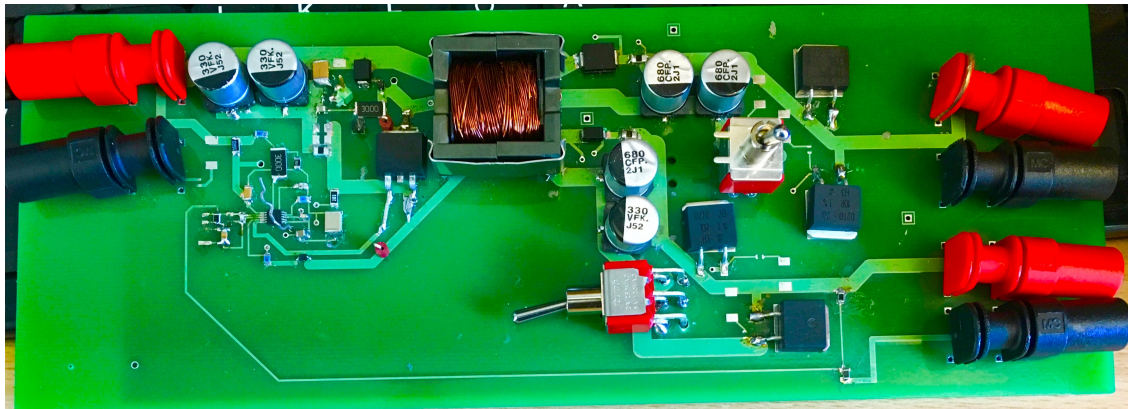




CHALMERS
UNIVERSITY OF TECHNOLOGY



Analysis and Design of Multioutput Flyback Converter

A study For A Lab Upgrade on the Flyback converter assignment at Chalmers Elteknik

Master's thesis in Electric Power Engineering

Abdi Ahmed
Abdullahi Kosar

MASTER'S THESIS 2016:ENM

Analysis and Design of Multioutput Flyback Converter

A study For A Lab Upgrade on the Flyback converter assignment
at Chalmers Elteknik

ABDI AHMED
ABDULLAHI KOSAR



CHALMERS
UNIVERSITY OF TECHNOLOGY

Department of Energy & Environment
Division of Electric Power Engineering
CHALMERS UNIVERSITY OF TECHNOLOGY
Gothenburg, Sweden 2016

Analysis and Design of Multioutput Flyback Converter
Master's thesis 2016:ENM
ABDI AHMED
ABDULLAHI KOSAR

© ABDI AHMED
ABDULLAHI KOSAR, 2016.

Department of Energy & Environment
Division of Electric Power Engineering
Chalmers University of Technology
SE-412 96 Gothenburg
Sweden
Telephone +46 (0)31-772 1000

Cover:
Multi-output flyback converter prototype PCB

Chalmers Reproservice
Gothenburg 2016

Analysis and Design of Multioutput Flyback Converter

Master's thesis 2016:ENM

ABDI AHMED

ABDULLAHI KOSAR

Department of Energy & Environment

Division of Electric Power Engineering

Chalmers University of Technology

Abstract

This thesis work is done in order to improve the existing lab in Chalmers for the study of Power Electronics. Assignments for the practical lab and computer simulation sessions of a flyback converter have been reviewed and analysed. The analyses of the existing assignments shows that the circuit board used in the lab today is a multi purpose circuit and it is difficult to relate a equivalent circuit diagram of a flyback converter. Furthermore, there is no relationship between the circuit and the simulation model.

A simulation was done using PSpice and a prototype PCB board built with the aim of showing some of these interesting concepts in the course. The main suggestions are related to the simplification of the circuits so that immediate correlation can be made between the circuits being shown in the class and the PCB used in the lab. The simulation model can be used in the simulation session of the course.

The new simulation model and the circuit board can demonstrate the role of the inductor in the flyback transformer by varying its value. Another area of improvement would be on demonstrating of magnetics theory. There is no simulation or practical assignments about magnetics in the course today. Understanding the relation between the current ripple and magnetic flux is in the scope of the courses. It is also important to understand how high frequency affects the losses and the size of the core. Two transformers are designed in order to investigate these relationships. The result of the transformer design shows that a new assignment that can demonstrate how magnetic core behaves can be introduced.

Keywords: Flyback, Multi-output, DCM,CCM, LM5020,Switch mode power supply

Acknowledgement

First of all we would like to thank the Almighty for making this possible. The contributions we had from our supervisor Andreas Henriksson were numerous and immeasurable and we would like to acknowledge his commitment and effort in enabling this work. Of notable mention is Altran, Ericsson and Chalmers who were the collaborating partners.

Encouragement and support from our family members and friends will not go unappreciated. Thank you.

Finally, Abdullahi would like to acknowledge the Swedish Institute for the generous scholarship for his master's studies.

Abdi & Abdullahi
Gothenburg, September 27, 2016

Contents

Abstract	v
Acknowledgments	vii
Contents	ix
List of Figures	xi
List of Tables	xiv
Abbreviations	xv
1 Introduction	1
1.1 Background	1
1.2 Problem	2
1.3 Purpose	3
1.4 Scope	3
2 Pedagogic Background	5
2.1 Existing Flyback Lab for ENM060	6
2.2 Existing Simulation Task for flyback in ENM060	7
2.3 Suggestions	8
3 Technical Background	11
3.1 Circuit Description	12
3.2 Operating Modes	13
3.2.1 CCM mode of operation	14
3.2.2 DCM mode of operation	16
3.2.3 Boundary between CCM and DCM	18

3.3	Magnetics	20
3.3.1	Characteristic of a magnetic core	21
3.3.2	Effect of Air gap	23
3.4	Control circuit of the flyback	24
4	Design and simulation of the model	27
4.1	System specifications	27
4.2	Determination of Maximum duty ratio (D_{max})	29
4.3	Transformers primary inductance (L_m)	31
4.4	Core selection	32
4.4.1	Determine the maximum flux swing (ΔB_{max})	36
4.4.2	Calculate windows area product AP	36
4.4.3	Determine the required number of minimum primary turns N_p^{min}	37
4.5	Determining the Secondary Turns	37
4.6	Determining the Wire Diameter	39
4.7	Choosing the diodes	40
4.8	Determine the output capacitors	41
4.9	Design of Clamp and Damping circuit	42
4.10	Compensator Design	44
5	Simulation and PCB Design of a Flyback	47
5.1	Existing Simulation Model	47
5.2	Proposed Simulation Model	48
5.3	PCB Design	49
5.3.1	Current Measuring	51
6	Simulations and Measurements	53
6.1	Simulations	53
6.1.1	Inductance value in CCM	53
6.1.2	Inductance value in DCM	54
6.1.3	Current sense simulations	55
6.1.4	Compensation Network	56
6.2	Measurements	57
7	Results	59
8	Discussion	63
9	Conclusion and Future Work	65
9.1	Conclusion	65
9.2	Future Work	66

Bibliography	68
A Derivations of the mathematical equations	A1
A.1 Converter	A1
A.2 Control	A2
A.3 Filter	A2
A.4 Matlab code for compensation network	A2
B Data sheets	A1
B.1 N87 datasheet	A1

List of Figures

3.1	Circuit diagram of the flyback converter	12
3.2	Equivalent Circuit of flyback converter.(a) When the switch is on and the diode is blocking.(b) When the diode is forward biased and the switch is off.	13
3.3	Voltage and current wave forms of flyback converter working on CCM	14
3.4	Current and Voltage wave forms of the flyback converter working in DCM.	17
3.5	Voltage and current wave forms of a flyback converter working on BCM	18
3.6	Normalized output current I_o at the boundary as a function of duty cycle (D) for a flyback converter.	20
3.7	Relationships between the electrical and magnetic quantities	20
3.8	B-H loop	22
3.9	Hysteresis in the B-H plane for ferromagnetic cores. Dashed line; with air-gap Solid line;with no air-gap	24
3.10	Type II error amplifier	26
4.1	flow chart of design procedure[1]	28
4.2	Switch and diode utilization factor versus duty cycle of a flyback. .	30
4.3	Relative core losses versus frequency for N87 core material	34
4.4	Primary inductor mode current, blue for DCM and red for CCM . .	35
4.5	Hysteresis in the B-H plane for ferromagnetic cores.(a) typical flyback operating in CCM.(b) typical flyback operating in DCM . . .	35
4.6	An ideal diagram of the transformer	38
4.7	(a)Output capacitor current.(b) Simple circuit diagram of the output capacitor, diode and load	42
4.8	Circuit showing the arrangement of a TVS and diode to achieve clamping	43

4.9	Voltage across the MOSFET: (a) Without clamp (b) With clamp (c) with clamp and damping resistance and capacitor	43
4.10	Equivalent circuit of a flyback converter.(a) ON mode (b) OFF mode.	44
4.11	Theoretical bode plot of the system	45
5.1	The existing simulation model.	47
5.2	Simulation model of a flyback converter with two outputs	48
5.3	Top Silkscreen	50
5.4	Top copper trace	51
5.5	Bottom Copper	51
6.1	Simulation: Current waveforms in a flyback converter operating in CCM mode with different input voltages: (a) $V_d=15$ (b) $V_d=30$. . .	54
6.2	Current waveforms in a flyback converter operating in DCM mode with different input voltages: (a) $V_d=30$ (b) $V_d=15$	55
6.3	Simulation: Current waveforms in a flyback converter operating in DCM mode with different input voltages: (a) $V_d=15$ (b) $V_d=30$. . .	56
6.4	Current measurement in the simulation model	56
6.5	Transient response of the output voltage: (a) When load-step is applied at input 1 (b) When load-step applied at input 2	57
6.6	Measured result	58
6.7	Drain Voltage with lower inductance value	58
7.1	Overview of the circuit board compared to the circuit diagram of the flyback converter.	60
7.2	Overview of two transformer with two different frequencies. The frequency of the large and small transformers are 65 and 300 kHz respectively	61

List of Tables

4.1	System specification	29
4.2	The RMS value of the current and the resulting primary inductance	32
4.3	Core list and design properties	33
4.4	Number of turns and core type	38
4.5	Copper diameter and their current carrying capacity for different A/cm^2	40
4.6	Rms value of the current and the required number of wires	40
4.7	Ratings of the power stage components	42

1

Introduction

1.1 Background

Power electronic converters is a common object in today's electronic world and for a very good reason. With quite a bit of interest in smaller sized consumer products and energy efficiency, there is a need for power supplies to adapt to these needs. The evolution of power supplies, as does many other electronic items, follows a trend that ends up with better and more efficient designs.

The need to control power more efficiently and reduce losses coupled with the improvement and advancement of power electronic switches led to the adoption of switched mode power supplies (SMPS). The main principle being that the input is connected to the energy storage devices (capacitors and inductors) only as long as it is required; not all the time as is with the case of linear regulators. Power electronic switches that can be switched as fast as several MHz enables this.

A switch mode power supply has a high efficiency which reaches up to 90 %. The high efficiency eliminates the need for big heat sinks and therefore the size and cost of the power supply decreases significantly. For this reason, a SMPS is preferred to use in situations where a high supply efficiency is necessary [2]. Some of the areas where this technology is applicable is in battery-powered and hand-held applications where the battery lifetime and the temperature are essential [3]. The disadvantages of an SMPS are minor and can be overcome with a proper design. However, switched mode power supply design is inherently a time consuming job requiring many trade-offs and a large number of design variables.

Power electronics is one of the four major areas taught to electrical power engineering students at Chalmers University of Technology. The main reason being that it

is an area that has wide applications and require some level of familiarity to future electrical engineers. Two courses (Power Electronic Converters (*ENM060*) and Power Electronic Devices and Applications (*ENM070*) deal with a wide range of applications in terms of power and the students carry out lab activities in these two courses. The aim of this thesis is to upgrade the lab exercises and the equipment used in these labs ,in particular the practical lab for the flyback converter.

There are several reasons that make it necessary to upgrade the current lab equipment. The lectures are based on simplified circuits while the existing circuit board contains many more components making the correlation difficult for the students. From a pedagogical point of view, it would be easier for the students to have a simple circuit with fewer components on it. Therefore, it is proposed in this report to design a simple flyback converter which can be easily compared to the material shown in the lectures. Another important demonstration will be to show the effects of different switching frequencies. The size of a switching power supply decreases as the switching frequency increases, but a high frequency also comes with high switching losses. In this thesis it is proposed to design two converters each with a different switching frequency to give the students an insight into how the frequency affects the different design parameters.

1.2 Problem

The laboratory sessions are aimed at giving a practical glimpse of some of the concepts that have been discussed in the lectures. The aim being, especially in the introductory courses, to give the student appreciation of some of the most important elements in the course. The laboratory exercise should give the student the possibility to see the concepts come to life without necessarily bogging the student down with details. It should however not abstract the workings so much as to turn it into another theoretical exercise. A fine balance has thus to be struck between simplicity and function.

The introductory elements which are most important to show in a practical lab and the best laboratory arrangement that is able to show these fundamental concepts is the aim of this thesis.

1.3 Purpose

The purpose of this thesis is to investigate the lab tasks that could be interesting for the students and the best way to link the lectures to the lab. A prototype circuit will be built in an attempt to show some of the interesting concepts in the study of power electronics. The thesis specifically deals with investigating a multiple output flyback converter. The design task will be to come up with a circuit that will display some of the fundamentals of a flyback converter. The design will first be done by calculations, then simulated and finally a working circuit will be created, tested and characterized.

1.4 Scope

The design task will be aimed at coming up with a working model that can display some of the most important fundamentals. Due to the nature of the the thesis, optimizations with regards to losses and EMI will not be a priority. There are also limitations in regards to the existing power supply in the lab which also sets a limit on the maximum size of the converter that is to be built. The existing power supply in the lab is rated 30V/2.5A which sets the limit for the flyback design.

The design will feature a multiple output design with one of the outputs being the master. There are many ways to achieve cross regulation and this thesis will not be overly interested with stabilizing the slave output beyond setting a large design margin.

The feedback will not be isolated since it requires other components such as an optocoupler. The design will be as simple as possible and the use of non-isolated feedback for this particular task will be safe due to the low power range of the converter.

The choice of control strategy between voltage and current control will be based on the chosen controller. In this design, current mode control will be chosen and the choice is motivated through the choice of controller.

2

Pedagogic Background

There are two power electronic courses in the first year of the masters program of electric power engineering at Chalmers University of Technology. The first course is power electronic converters (ENM060) and the aim of the course is to give students the basic knowledge about the operating principles of the most common power electronic converter topologies. Basic converter design, analysis of the wave-shapes and efficiency calculations are among items that are covered in this course. Besides the lectures and demonstrations, there are 7 PSpice simulation tasks and two practical labs. Two of these simulations assignments are related to DC/DC converters, one for Boost and Buck converters and the other one for flyback converters. In addition to this, there are two practical labs where the first lab covers the operating principle of a buck converter and the second lab is intended to demonstrate the operating principle of the flyback converter. However, this report will focus only on the flyback converter. Therefore, in this chapter the existing simulation model and the practical lab of the flyback converter will be reviewed.

The ENM060 course also lays the foundation for the continuation course Power Electronic Devices and Applications (ENM070). The topics that are related to the DC/DC converters which this course covers are:

- Gate and drive circuits
- Snubber circuits
- Control circuits for DC/DC-converters.

In the ENM070 course, there is a practical lab-project which covers the above stated subjects and a circuit board of flyback converter is available in the lab. This circuit board is poorly designed in terms of drive circuits, snubber circuits and the

compensation network of the circuit. The idea with the lab is to modify the design of a flyback converter to achieve better performance. The existing assignments in this lab are relevant to the aim of the course and they cover the above stated points. However, currently there is no simulation model available which would give the students more space to carry out different experiments and make it easier to study the converter behaviour. By simulating the circuit, students can optimize their solutions and therefore, this project is suggesting a new circuit board with a corresponding simulation model which can be implemented in the existing lab assignments.

2.1 Existing Flyback Lab for ENM060

The practical lab of the ENM060 course consists of two parts. The first part is a homework assignment in which the students prepare some theoretical calculations. This part focuses on the following points:

- Calculation of the magnetizing inductance (L_m) value from the core parameters; the air gap (l_g), relative permeability (μ_r) and the area of the core (A_e).
- Drawing of the wave forms of the current and voltage if the load resistance and duty cycle are fixed and the frequency has two different values. This shows how the wave forms change when the frequency is changed.
- Deriving the transfer function of the voltage and current in different conduction mode.

In the lab there are 7 tasks which are intended to verify the theoretically calculations. These tasks can be arranged as follows:

- The first task is to calculate the magnetizing inductance from the wave forms and the duty cycle. The energy needed to be transferred by the converter is directly proportional to the inductance and by knowing the frequency and the input power, the transferred energy can be calculated. The value of the magnetizing inductance L_m is compared to the inductance value calculated from the core parameters in the home assignment. This is one way to show the relationship between the value of the magnetizing inductance and the energy stored in the core.
- Task two and three deal with how to verify the calculated values of the voltage over the power switches and the current through them by comparing the waveforms calculated in the home assignment with the measured curves.

- In task four, the efficiency of the converter is calculated in three different operating points which demonstrates how the efficiency of the converter changes if the loading condition of the converter changes.
- One of the operation principles of the open loop flyback converter is that the output voltage becomes very high if the converter is lightly loaded. The output voltage can be restricted to a reasonable level by adding one more winding in the transformer. This task is intended to demonstrate the benefit of a third winding in the transformer.
- The other tasks are not directly connected to the home assignments. They show the importance of the snubber circuits and the difference between two diodes. One diode with high voltage drop but good switching characteristics that can be switched off quickly and another diode with low voltage drop and poor switching characteristics.

2.2 Existing Simulation Task for flyback in ENM060

The aim of the Pspice simulation in ENM060 is to analyze and perform analytic calculations of an ideal flyback DC/DC converter. The operating principle of this topology is thoroughly evaluated in both continuous and discontinuous conduction mode by its current and voltage waveforms. As for the practical lab, the Pspice assignment consists of two parts. The first part is to derive the theoretical calculations and consists of the following tasks:

- Derivation of the transfer function of a flyback converter operating in CCM.
- Theoretical calculation of the ripple in the magnetizing current Δi_m
- Derivation of a transfer function for a flyback converter operating in DCM.

After the theoretical calculation of the wave forms and the transfer function of the flyback converter, the students shall simulate and verify the results from the theoretical calculations. In this part, the following points are focused on:

- Study the wave forms of the converter in both continuous and discontinuous conduction mode.
- Verify that the load resistance has no impact on the transfer function between the input and output voltages if the converter is working in continuous conduction mode.

- To demonstrate that the converter will move from CCM to DCM if the load resistance increases.

The other tasks are not directly related to the home assignments but demonstrate the advantages of the third winding in the transformer and the need for snubber circuits.

2.3 Suggestions

1. The first task in the practical lab is to study the circuit board and locate the main components of the flyback converter. Since the circuit board is a multipurpose board, it is not an easy task to understand the function of every part on the board. The students may mistakenly think that it is important to use all parts on the board in order to get the flyback converter to function. Therefore, it is suggested to design a simple flyback converter in which the different components of the converter can be easily identified.
2. As mentioned in chapter one, the operating frequency of the SMPS has a huge impact on the size and the efficiency of the converter. To demonstrate this relationship, two flyback transformers will be designed that are working with two different switching frequencies (65 kHz and 300 kHz). Designing of a flyback transformer can be also a good exercises for students to understand the basics of the magnetics. Therefore, a flyback transformer is designed in this theses, in order to investigate if it is suitable that the students can design a transformer during the course.
3. One of the advantages of a flyback converter is the possibility to have several outputs. For this reason, the proposed flyback converters will have two outputs.
4. Apart from the design of the new flyback converters, this project is suggesting to make the following improvements for the existing tasks of the practical lab and the Pspice simulation model:
 - A simple simulation model which clearly shows the functionality of the flyback converter. The transformer should be model as an ideal transformer in parallel with the inductor.
 - The simulation model should be a close loop system in which students can design the control parameters of the system.
5. One more important thing to understand is that a typical converter is usually

designed to operate in either CCM or DCM. It is therefore import to calculate the magnetizing inductance which can guarantee CCM or DCM depending on the designers choice. It is essential to understand how to calculate the critical inductance value which gives the decided conduction mode in all conditions. An assignment can be that the students should calculate the inductance value which gives CCM or DCM and let students insert this value in the Pspice simulation to verify that the theoretical calculation holds.

3

Technical Background

The design of a flyback converter requires a wide understanding of a variety of components and disciplines. The problems that have to be dealt with during the design process are for instance, magnetics, control loop analysis and power devices such as switches, capacitors, and transformers. Therefore, a theoretical review of the operating principle of a flyback converter, circuit description and operation modes is done. Magnetics and control theory are also covered.

The input voltage of a DC/DC converter is typically unregulated and the converter is used to convert the unregulated voltage to a controllable voltage level [3][4]. A DC/DC converter can be used with or without electrical isolation depending on the application. The flyback converter is classified as an isolated converter since there is electrical separation between the input and output. One of the main reasons for the isolation is to prevent the user from electric shock since the input voltage can be hazardous. The isolation is achieved by adding a transformer to the basic buck-boost converter. The operating principle of the Buck-boost converter is not included in the scope of this project, but a good explanation of this converter is provided in [4],[5] and [6].

A flyback converter is a good choice for a robust design in the range of 20W to 200W [5]. This is due to the low number of components required in this type of converter. Another advantage of the flyback converter is the possibility to have several outputs which makes it very useful for applications where different voltage levels are needed such as computers, TVs and other electronic equipment [5].

Fig 3.1 shows the basic circuit diagram of a multiple output flyback converter. The main power stage is the part that transfers energy and consists of the transformer, the primary switching MOSFET (Q_1), secondary rectifiers (D_1 and D_2) and the input and output capacitors. The control circuit drives the switch Q_1 with a fixed

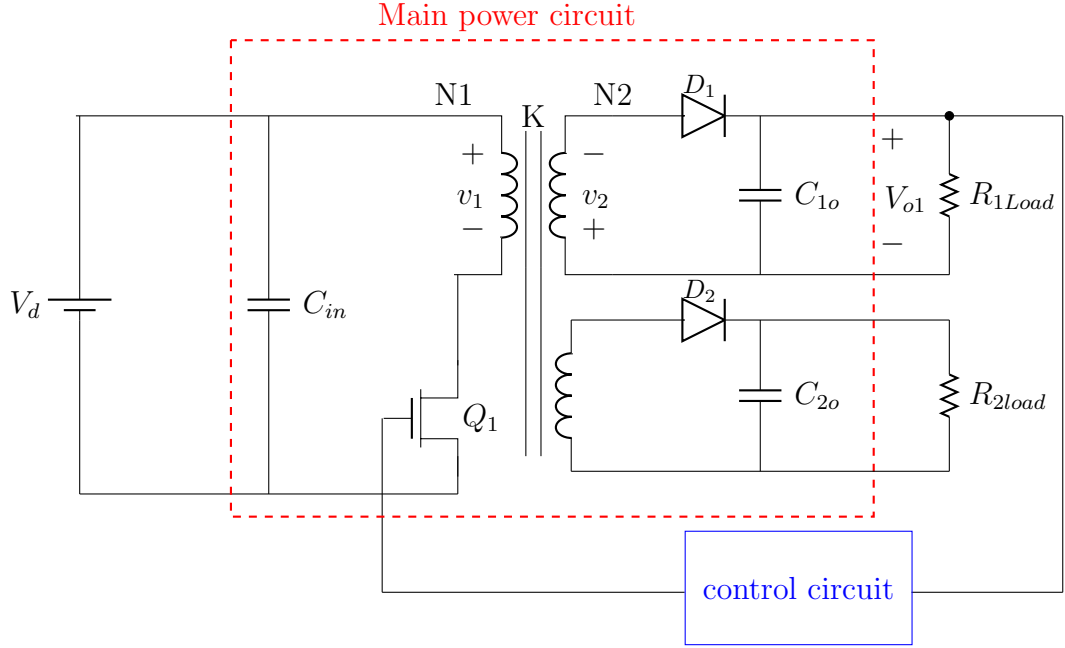


Fig. 3.1: Circuit diagram of the flyback converter

frequency and regulates the master output voltage V_{o1} against any line and load changes [4] while the slave voltages are unregulated [2].

3.1 Circuit Description

The power circuit consists of the power switch Q_1 , the diode and the transformer. For description purposes, the equivalent circuit diagram of a single output flyback converter will be analysed as shown in Fig 3.2. When the switch is conducting during t_{on} the diode is blocking as seen in Fig 3.2(a). This has to do with the nature of the transformer, when a current i_d flows into the dot at primary side, it flows out of the dot end of the secondary, which makes the diode reverse biased. When the switch is off, the diode is forward biased and starts to conduct. Since the secondary and primary sides of the flyback transformer are not conducting simultaneously, the transformer behaves as a two winding inductor. [2][7][4].

The transformer of the converter is modelled with a simple equivalent circuit consisting of an ideal transformer in parallel with a magnetising inductance L_m as shown in Fig 3.2. The function of the primary inductance L_m is to store magnetic energy provided from the source V_d . When the diode D starts to conduct, this stored energy is transferred to the load with inductance voltage and current scaled

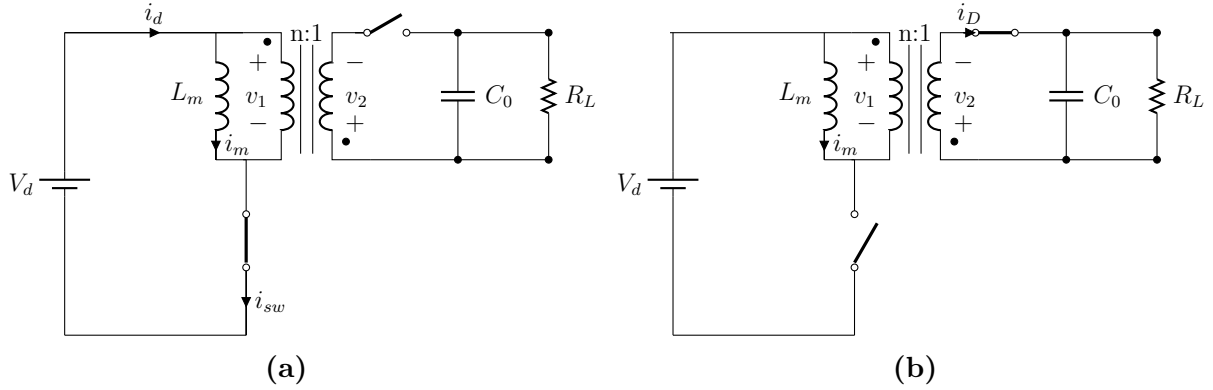


Fig. 3.2: Equivalent Circuit of flyback converter. (a) When the switch is on and the diode is blocking. (b) When the diode is forward biased and the switch is off.

according to the turns ratio of the transformer [5]. In order to get a smooth current at the output a capacitor is applied on the secondary side of the transformer [2]. The capacitor should be big enough to store enough energy during t_{on} in order to supply the required energy to the load when the diode is not conducting.

3.2 Operating Modes

Like other converters a flyback converter has two operating modes; continuous conduction mode (CCM) and discontinuous conduction mode (DCM). The two operation modes have different transfer equations and different current and voltage wave forms. Therefore, from a design point of view it is important to analyse the current and voltage that the electric components in the converter experience. Particularly the current flowing through the circuit, voltage across the switch and the diode [2]. The magnetizing inductance and the load current determines the operation mode of the converter.

During the analysis of the different conduction modes of the converter, the following assumptions will be made [5].

- The converter is operating in steady state
- The converter is ideal, that is the input power is equal to the output power
- Leakage inductance, stray capacitors and stray resistances are neglected.

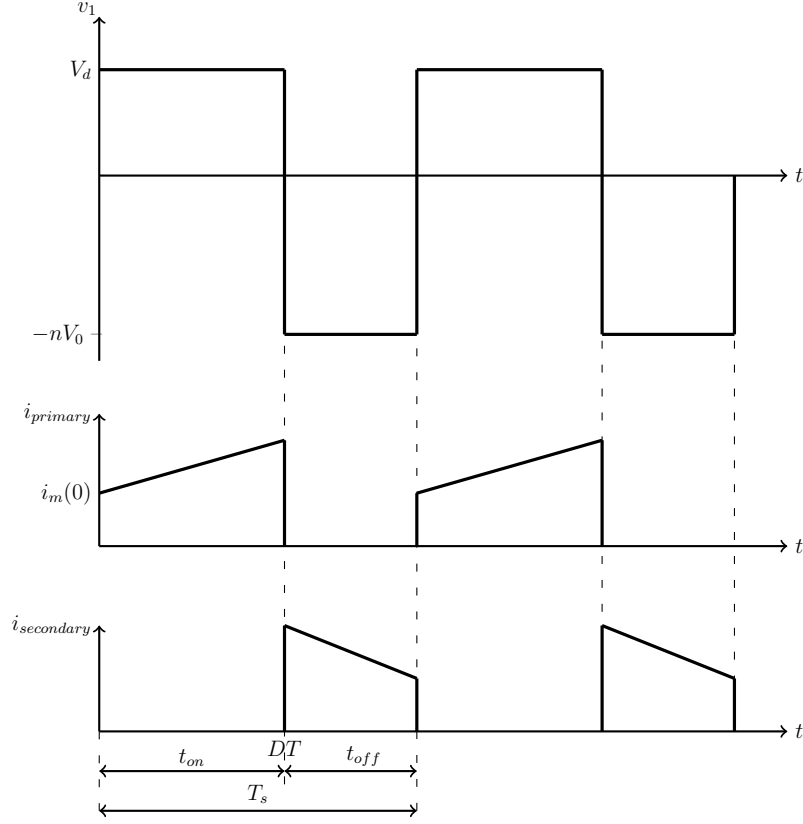


Fig. 3.3: Voltage and current wave forms of flyback converter working on CCM

3.2.1 CCM mode of operation

For this operation mode, the energy stored in the core during t_{on} is not fully dissipated during t_{off} . The current and voltage waveforms of this conduction mode are shown in Fig 3.3.

When the switch Q_1 starts to conduct, the current that flows through the magnetising inductance increases linearly due to the constant input voltage V_d [8]. It is important to know the peak and the ripple value of the magnetising current, since the losses in the transformer, filters and the power switches are related to the peak and RMS value of this current [5]. The magnetising current i_m during t_{on} can be expressed as

$$i_m(t) = \frac{V_d}{L_m}t + i_m(0) \quad (3.1)$$

where L_m is the magnetising inductance and $i_m(0)$ is the initial value of the primary

current when the switch starts to conduct. The peak value of the current occurs at $t = DT$ which is calculated as

$$i_m(DT) = \frac{V_d DT}{L_m} + i_m(0) \quad (3.2)$$

and the ripple current of the primary is

$$\Delta i_m = i_m(DT) - i_m(0) = \frac{V_d DT}{L_m}. \quad (3.3)$$

As shown in Fig 3.3, when the diode starts to conduct at $t = DT$ the primary current transfers to the secondary with the amplitude $I_s = nI_p$, where n is the transformer turns ratio [2]. The current flowing through the magnetising inductance (i_m) cannot change instantaneously, therefore the magnetising inductance will put up a negative voltage to drive this current. As shown in Fig 3.2, the magnetising inductance is in parallel with the primary side of the ideal transformer and therefore the transformer changes polarity which forces the diode to conduct. The voltage that appears across the switch becomes

$$V_{sw} = V_d - v_1 = V_d - (-nV_o) = V_d + nV_o \quad (3.4)$$

where $-nV_o$ is the output voltage reflected to the primary side of the transformer. Due to the constant negative value of the voltage, the current through the diode decreases linearly [4]. The diode current during this period is

$$i_D = i_m = i_m(DT) - \frac{V_o(1-D)T}{L_m} \quad (3.5)$$

where $i_m(DT)$ is the initial value of the magnetising current when the diode starts to conduct and i_D is the current through the diode. The average value of i_D is equal to the output current I_o and as seen from Fig 3.3, the duty cycle varies as I_o changes. Therefore, the output current is simply the average of the diode current which becomes

$$I_D = \frac{I_o}{1-D}. \quad (3.6)$$

This current which flows through the switch during t_{on} is reflected to the secondary side and can be expressed as

$$I_{sw} = \frac{1}{n} \frac{I_o}{1 - D}. \quad (3.7)$$

It can be observed from (3.6) and (3.7) that the maximum I_{sw} and I_o is dependent on the maximum duty cycle.

The transfer function of the voltage can be derived from a a loss-less converter. The input and output power are equal which gives,

$$I_o V_o = V_d I_d \quad (3.8)$$

where the product of V_d and I_d is the power drawn from the source. The mean voltage across the magnetising inductance is zero during one period [8] which means that the volt-second area during the on time is equal to the volt-second area during the off time

$$V_d D T = n V_o (D - 1) T. \quad (3.9)$$

Therefore, the transfer function of the converter becomes

$$\frac{V_o}{V_1} = \frac{I_1}{I_o} = \frac{1}{n} \frac{D}{D - 1}. \quad (3.10)$$

3.2.2 DCM mode of operation

This mode of operation occurs when the energy stored in the transformer is completely depleted in a single cycle. Fig 3.4 shows the current and voltage wave forms of a flyback converter operating in DCM. The magnetising current behaves as in CCM and can still be expressed with (3.1) except the initial condition of the current $i_m(0)$ is zero in this case because all energy in the core has been dissipated during t_{off} of the previous cycle [3]. Since the current starts from zero, a high peak current is required to deliver the required output power. This means that in this operating mode, the RMS value of the current is higher than in CCM and consequently the losses in the MOSFET, the transformer windings and the capacitors become higher [9]. On the other hand, the high ripple current results in higher magnetic flux swing (ΔB) which is proportional to the losses in the core as explained in section 3.3.1.

According to (3.13) the transfer function of this operation mode is not only dependent on the duty cycle but also on the dead time ΔT_s which is when the current

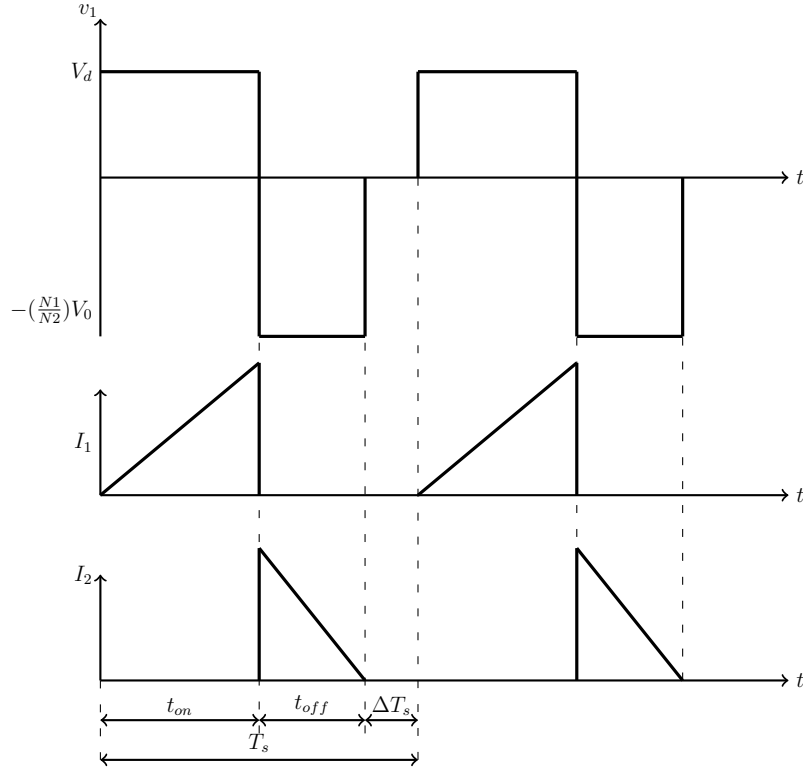


Fig. 3.4: Current and Voltage wave forms of the flyback converter working in DCM.

through the magnetising inductance is zero. For the CCM case, the relationship between i_D and I_o only depend on the duty cycle according to (3.6) whereas for DCM it becomes

$$I_o = \frac{D_1 i_D}{2} = \frac{D_1}{2L_m} \int_{DT}^{D+D_1} nV_o dt = \frac{nV_o D_1^2 T}{2L_m} \quad (3.11)$$

where $D_1 T$ is the time that the energy stored in the magnetising inductance is completely discharged and nV_o is the reflected voltage. According to the volt-second balance of the inductor, the relationship between the input and the output voltage can be expressed as

$$\frac{V_o}{V_d} = \frac{I_1}{I_o} = \frac{1}{n} \frac{D}{D_1}. \quad (3.12)$$

The output voltage and current are a function of D_1 and duty cycle D according to (3.12) which complicates the design of the control loop in DCM. However, it is

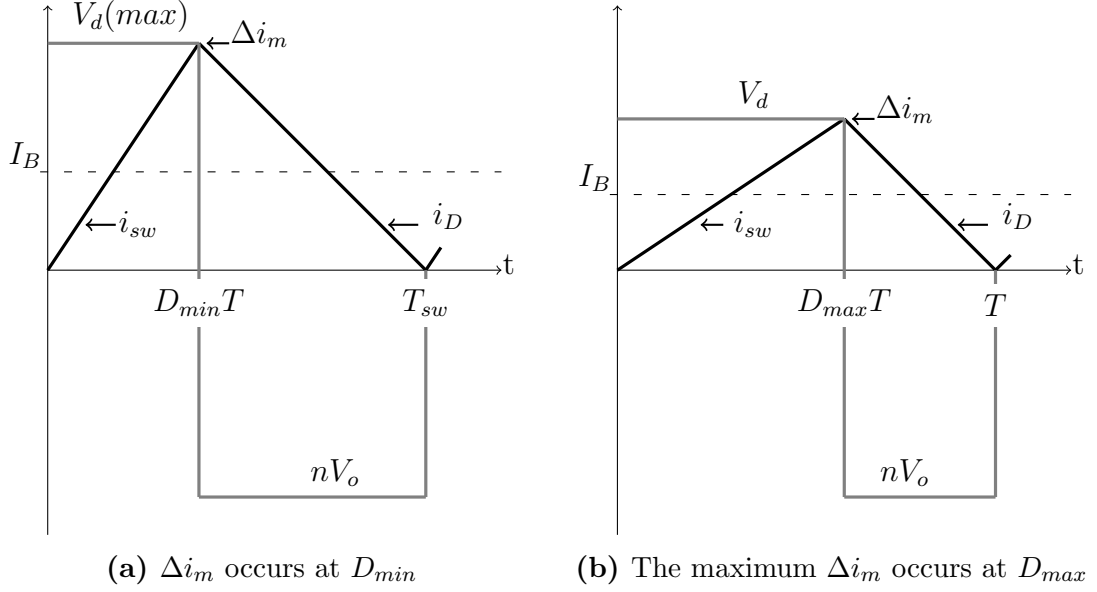


Fig. 3.5: Voltage and current wave forms of a flyback converter working on BCM

quite normal to use the boundary condition equations. The final transfer function of a DCM flyback converter can be derived by combining (3.11) and (3.12)

$$\frac{V_0}{V_1} = \frac{I_1}{I_o} = D \sqrt{\frac{TR_L}{2L_m}} \quad (3.13)$$

3.2.3 Boundary between CCM and DCM

The boundary between CCM and DCM is when the switch starts to conduct at the instant that the current through the diode goes to zero [4]. The waveforms of the current and voltage for this operating point are shown in Fig 3.5. The figure shows two extreme points, when the input voltage is minimum and when it is maximum. The case shown in Fig 3.5 (a) is a critical point for a converter designed to operate in CCM. Assume that the voltage reaches its maximum value and cannot increase any further, the only parameter that can shift the system to DCM is the output current. The system will shift to DCM if I_o decreases beyond the value shown in the figure. On the other hand, the case shown in Fig 3.5 (b) is used as a design reference point when designing a converter intended to operate in DCM

According to (3.11), the output current can be expressed as

$$I_o = \frac{nV_o(1-D)^2}{2L_m f_s} \quad (3.14)$$

where the output current is a function of the output voltage, frequency, duty cycle and the primary inductance. The output voltage and frequency should be chosen according to the system requirements and the inductor value is a design factor which decides whether the converter operates in CCM or DCM. With a chosen inductor value, a converter can change the operation mode as the duty cycle or the output current changes. Fig 3.6 shows the normalised output current against the duty cycle which is expressed as

$$\frac{I_o 2L_m f_s}{nV_o} = (1-D)^2 \quad (3.15)$$

where f_s and V_o are fixed and L_m is chosen according to the desired operation mode of the converter. To ensure CCM in the worst case scenario where I_o and D are its minimum, a high inductance value should be chosen. If referring to Fig 3.6 and assuming that the converter operates at point (A), a decrease in duty cycle as shown by the arrows will lead to the eventual movement of the operating point to (B) at the boundary. At this point, any further reduction of duty cycle or output current will shift the system to DCM. Conversely, for the operating point (C) in DCM, an increase of the duty cycle will shift the system to the boundary (D). Any further increase in the duty cycle or output current will shift the mode of operation.

The voltage and current waveforms of the operating point (A) are shown in Fig 3.5(a). A flyback converter operating in CCM for all load and input voltage conditions should be designed to operate at point (A) while if operating in DCM it should be designed for point (B). From a pedagogical point of view, it is important to show both operating modes and therefore, the proposed converter in this thesis will be designed to operate in CCM but allowing it to move to DCM when the input voltage or the output current changes.

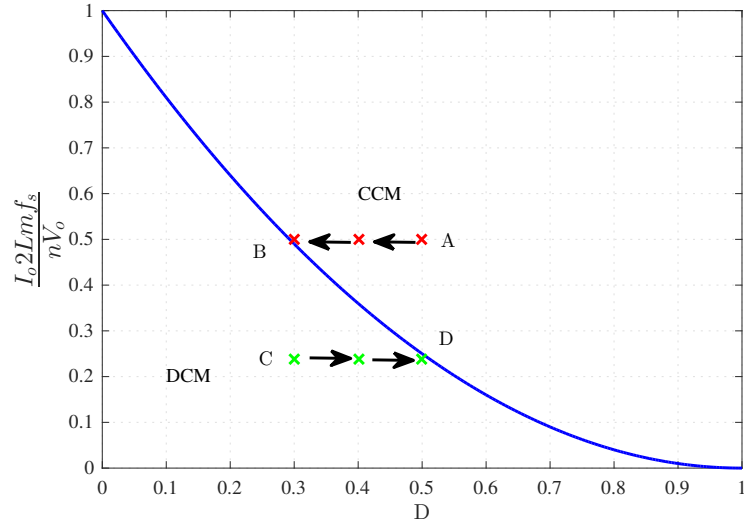


Fig. 3.6: Normalized output current I_o at the boundary as a function of duty cycle (D) for a flyback converter.

3.3 Magnetics

Magnetics are integral to switching converters as designing of transformers and inductors requires a basic knowledge of the subject. Fig 3.7 summarises the relationship between magnetic and electric parameters such as magnetic intensity H , magnetic flux density B , electric current and voltage.

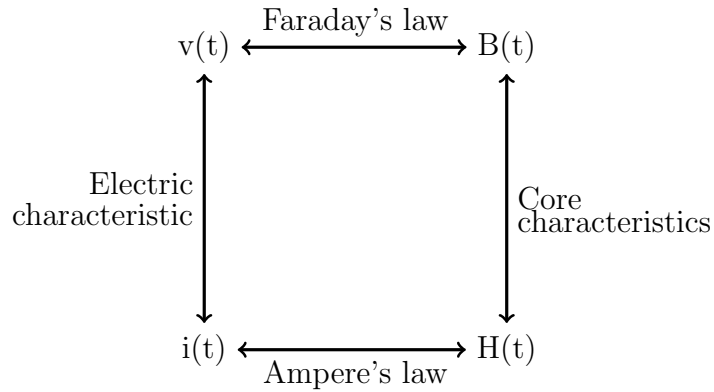


Fig. 3.7: Relationships between the electrical and magnetic quantities

The current relates to the magnetic field through Ampere's law which states that

the line integral of magnetic intensity (\mathbf{H}) around an enclosed path is equal to the total current that encloses that path [5] as

$$\oint \mathbf{H} \cdot d\mathbf{l} = Ni \quad (3.16)$$

where, N is the number of turns [5]. Faraday's law relates the voltage induced on the winding to the magnetic field intensity

$$v(t) = N \frac{d\phi}{dt} = N A_e \frac{d\mathbf{B}}{dt} \quad (3.17)$$

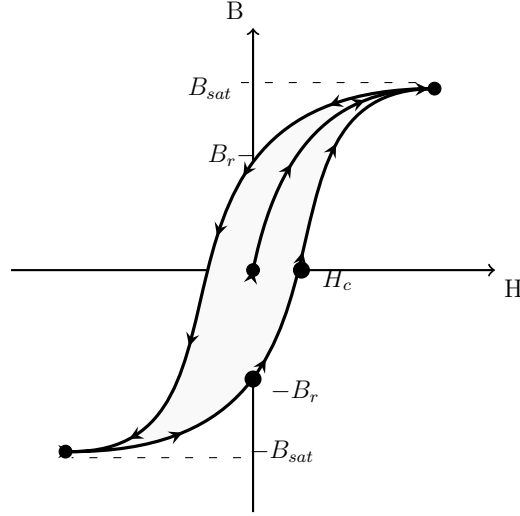
where ϕ is the magnetic flux passing through a surface with area A_e . The relationship between the magnetic intensity \mathbf{H} and the magnetic flux density \mathbf{B} is determined by the permeability of the core material [10] which can be expressed as

$$\mathbf{B} = \mu_o \mu_r \mathbf{H} \quad (3.18)$$

where μ_r is the relative permeability of the medium and μ_o is the permeability of free space. Most materials such as air, paper and copper, have a low relative permeability compared to ferromagnetic materials. For instance, μ_r of air is 1 while μ_r can reach up to 10^6 for ferromagnetic materials [10, 11]. In order to get a reasonable efficiency it is important to use materials that give low losses when the energy is being transformed from the electric to the magnetic domain or vice versa. For example, a ferromagnetic core material will amplify \mathbf{B} much better than a material with low permeability.

3.3.1 Characteristic of a magnetic core

The relationship between \mathbf{B} and \mathbf{H} is non-linear and dependent on the excitation waveforms and it is not possible to predict the shape of the \mathbf{B} - \mathbf{H} loop [12]. A complete cycle of magnetisation and demagnetisation of typical ferromagnetic core is shown Fig 3.8.

**Fig. 3.8:** B-H loop

Assuming that the excitation field intensity H is sinusoidal, the resulting magnetic flux becomes also sinusoidal. As H increases in the positive direction, B follows the arrows of the curve shown in Fig 3.8 which connects the origin and B_{sat} . When H starts to decrease to zero, B does not follow the previous curve and stays at B_r even when H becomes zero. This means a residual magnetic flux will be present in the material. The process continues when H goes negative and B will only be zero for a certain negative value of H required to get rid of the residual B . This deviation creates a hysteresis loop.

Hysteresis loops due to magnetising and demagnetising of the core materials represents energy losses per unit volume [12][10][13]. The energy loss for one complete cycle can be expressed as

$$W_{cycle} = V_{core} A_{BH} \quad (3.19)$$

where W_{cycle} is the energy loss per cycle, V_{core} is the volume of the core and A_{BH} is the area inside the BH-loop. The power loss is equal to the energy loss per cycle times the excitation frequency

$$P_{cycle} = f_s W_{cycle}. \quad (3.20)$$

In addition to the hysteresis losses, there are other losses in the core such as eddy current losses. One way to decrease the eddy losses is to use a core material with a high resistivity to prevent a high eddy current circulating in the core.

3.3.2 Effect of Air gap

The linearised hysteresis loop of a magnetic material can be modified by introducing an air gap in the core. The presence of an air gap in the core makes it possible to carry more current through the winding without risking saturating the core. The B-H characteristics shown in Fig 3.8 can be linearly modelled by neglecting the hysteresis loop as shown in Fig 3.9 which shows how an air gap inside a magnetic core affects the relation between the current and the magnetic flux. By reformulating (3.16) and (3.17), this relationship can be expressed as

$$\phi(\mathfrak{R}_m + \mathfrak{R}_g) = Ni \quad (3.21)$$

where \mathfrak{R}_m and \mathfrak{R}_g are the reluctance of the magnetic material and the air, respectively. The reluctance is inversely proportional to the permeability of the material in is

$$\mathfrak{R} = \frac{l}{\mu A} \quad (3.22)$$

where $\mu = \mu_r \mu_0$ and l and A are the mean path length and the cross-sectional area of the core, respectively. Fig 3.9 shows that when an air gap is present in the core, it will saturate with a higher current compared to the case with no air gap. This phenomena is in particular useful when designing a flyback. As described earlier, the transformer in the flyback is an energy storage device which stores and releases this energy for every cycle. Therefore, the energy stored in the transformer for every cycle of period can be increased by introducing an air gap. However, an air gap will also affect the value of the inductance. The relationship between the inductor and the reluctance can be derived from (3.21) and (3.17) which gives the inductance as

$$L = \frac{N^2}{\mathfrak{R}_m + \mathfrak{R}_g}. \quad (3.23)$$

It can be observed from (3.23) and (3.22) that the inductance is directly proportional to the permeability of the air and the magnetic materials. If there is no air gap and $\mathfrak{R}_g = 0$, then the inductance is just a function of the relative permeability μ_r of the core material which is a non linear parameter that is difficult to control. The permeability is dependent on the temperature, the magnetising history of the

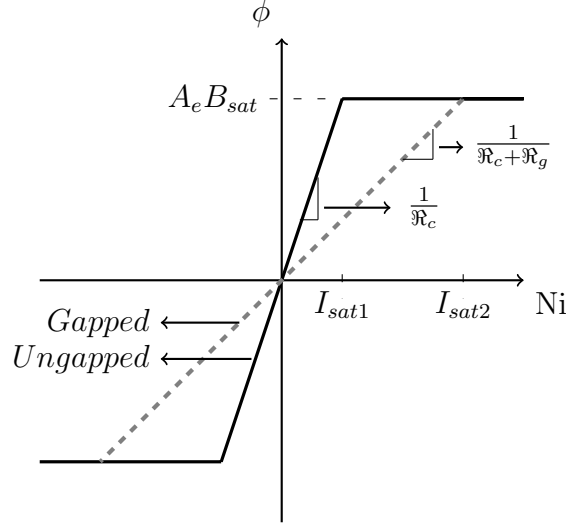


Fig. 3.9: Hysteresis in the B-H plane for ferromagnetic cores. Dashed line; with air-gap Solid line; with no air-gap

material and the location of the operating point and in turn, the inductance becomes difficult to control as well [11][12]. Therefore, another advantage of having an air gap is that it gives an possibility to control the inductance value.

3.4 Control circuit of the flyback

The overall transfer function of a converter is

$$T_{ol} = T_p T_c \quad (3.24)$$

where T_p is the transfer function of the power stage and T_c is the compensation network. Bode diagrams give an immediate overview of the stability of a circuit. In this case, one of the outputs of the converter is being controlled using a feedback loop to achieve a constant voltage. The feedback loop compares the actual output to the desired output and the controller takes corrective action by changing the duty cycle to make these two quantities equal.

In understanding a bode plot, two quantities are important. One of them is the DC gain and the other the phase margin. The DC gain is the gain at zero frequency and the aim should be to have this as high as possible in order to reduce static errors. The phase margin represents the phase difference between the control signal and the output at unity gain(0 dB). The aim is to have this at a minimum of 45° .

The compensation network should be designed to give us the required gain and phase margin of the total system. Depending on the needed phase boost, the error amplifier can be configured in three different classes.

Type I: This error amplifier is configured just to give a DC gain and no phase boost

Type II: When the phase margin is too low at the crossover frequency and lags down to negative 90°

Type III: When the phase lag goes to negative 180° instead, a type III error amplifier will do the job

Flyback converters that are operating in current mode, exhibit an open loop transfer function that requires a type II compensation network which consists of an integrator with high DC gain, a zero and a pole in the transfer function. The maximum boost occurs between the two frequencies where the zero and pole is placed. As seen in Fig 3.10, the gain and phase plot of the amplifier shows the integrator action that increases the gain and creates a phase boost. This type of network is realized by an operational amplifier with an impedance network of R_1 , C_1 and C_2 designed to introduce the poles and zeros at required frequencies.

The transfer function of the type II compensator becomes

$$T_c(s) = \frac{1 + sR_2C_1}{sR_1(C_1 + C_2)(1 + sR_2\frac{C_1C_2}{C_1+C_2})} \quad (3.25)$$

where R_2 and C_1 are used to set the location of the zero such that

$$w_z = \frac{1}{R_2C_1}. \quad (3.26)$$

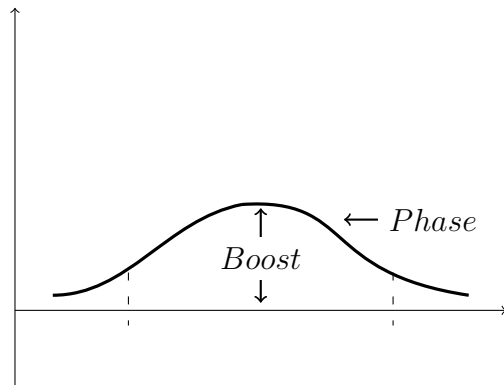
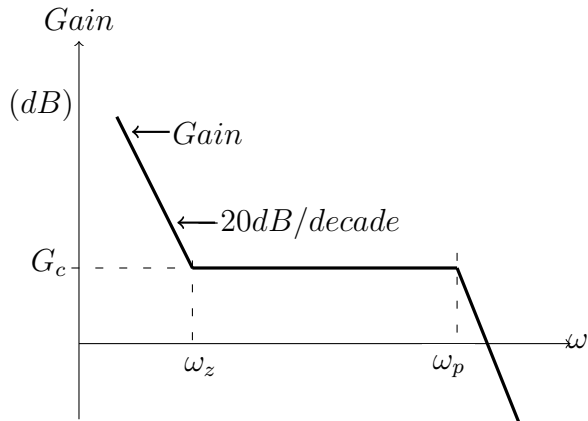
The pole at the origin (integrator) is set at

$$w_{p1} = \frac{1}{R_1(C_1 + C_2)} \quad (3.27)$$

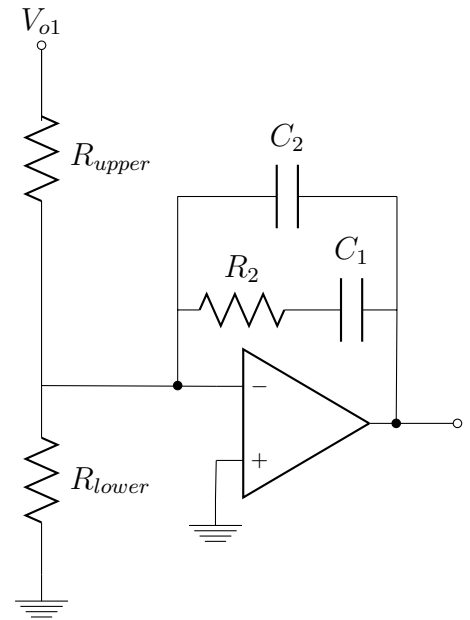
and the high frequency pole at

$$w_{p2} = \frac{1}{R_2\frac{C_1C_2}{C_1+C_2}}. \quad (3.28)$$

The poles and zero locations are then choosen to shape the compensation network. The capacitors and resistor are choosen using (3.25) to (3.28) which defines the desired transfer function of the converter.



(a) Gain and phase in log scale



(b) The error amplifier

Fig. 3.10: Type II error amplifier

4

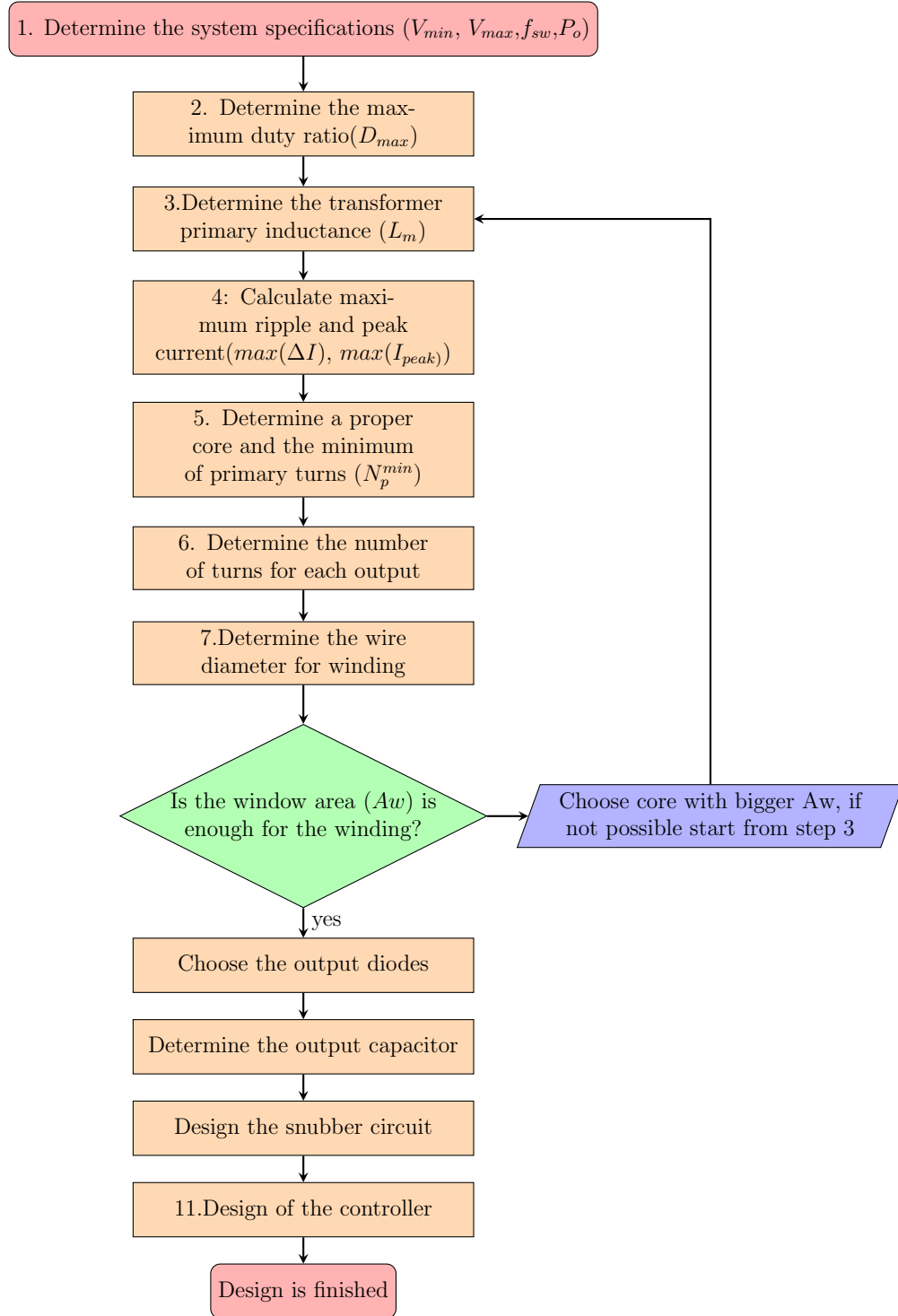
Design and simulation of the model

Designing of a SMPS is not an easy task and requires many trade-offs and considerations [3][1] and there are different design approaches that have been presented in [1][9][14]. There are several publications that provide good design examples [2][3][6][5][15]. However, all the examples presented deal with how to optimise a flyback converter for a specific operation point. These examples focuses on the design process of a flyback operating in either CCM or DCM. The purpose of this master thesis is to design a flyback converter which can operate both in CCM and DCM therefore the control system must be carefully analysed. For example, when the system shifts from DCM to CCM, its transfer function changes and a the Right Hand Plane Zero (RHPZ) due to the CCM may cause instability. To avoid such problems, the converter can be designed for CCM and shift operation to DCM at light load [9]. Fig 4.1 shows the design procedure used in this project

4.1 System specifications

The design procedure starts by determination the system requirements [2][9]. The input voltage is designed to be varied from 15 V to 30 V to show the different operation points. The efficiency is required to be estimated in order to calculate the input power according to

$$P_{in} = \frac{P_0}{\eta} \quad (4.1)$$

**Fig. 4.1:** flow chart of design procedure[1]

A typical flyback converter has an efficiency of around 0.8 ~0.85. The other system parameters that are essential for the design process are listed in Table 4.1. Note that two different values of switching frequencies are defined in Table 4.1.

Table 4.1: System specification

Parameters	Value	Description
P_o	20 W	Output power
I_{1o}	1 A	Load current
V_{1o}	10 V	Load voltage
I_{2o}	2 A	Load current
V_{2o}	5 V	Load voltage
f_{sw1}	65 kHz	Switching Frequency
f_{sw2}	300 kHz	Switching Frequency
$V_d(max)$	30 V	Maximum input voltage
$V_d(min)$	15 V	Minimum input Voltage
Efficiency(η)	80%	converter efficiency

4.2 Determination of Maximum duty ratio (D_{max})

In many cases the maximum duty cycle ratio is limited by the controller circuit which can typically be 50%. However, it is important to understand how the maximum duty cycle affects the voltage and current ratings of the MOSFET and the diode which are correlated with the losses in the converter. The voltage across the switch is expressed by (3.4) and (3.10) gives the relationship between the input voltage (V_d) and the output voltage V_o . Rearranging these two equations gives the voltage across the switch as a function of the duty cycle

$$V_{sw} = \frac{V_d}{1 - D}. \quad (4.2)$$

The average current through the diode is expressed in (3.6) which when referred to the primary side gives

$$I_p = \frac{P_{in}}{(V_d - V_{ds})D} \quad (4.3)$$

where P_{in} is the input power and V_{ds} is the voltage drop across the switch. It can be observed from (4.2), (4.3) and (3.6) that any selected value of D_{max} has an impact on the voltage and current that the diode and switch experience. Thus, the optimum diode and switch utilisation is characterised by the output power capability (C_p) of the flyback converter[5] which can be expressed as

$$C_p = \frac{P_o}{P_{sw}} = \frac{V_o I_o}{V_{sw} I_{sw}}. \quad (4.4)$$

The relationship between I_{sw} and I_o is given by (3.6) while V_{sw} can be related to V_o through (4.2) and (3.10) which gives

$$C_p = \frac{V_o I_o}{\frac{I_o}{n(1-D)} \frac{nV_o}{D}} = D(1 - D) \quad (4.5)$$

where D varies between 1 and 0. Fig. 4.2 shows C_p versus the duty cycle and as seen from the figure, C_p increases from zero as D increases and reaches its maximum value when $D = 0.5$ and finally decreasing to zero when D is 1. This means the switch power P_{sw} is minimum when $D=0.5$.

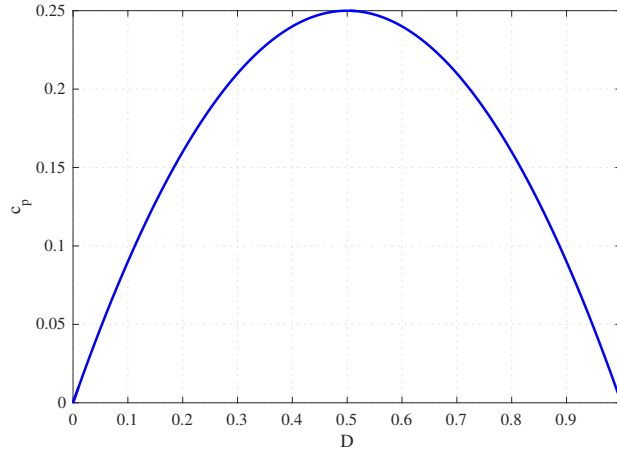


Fig. 4.2: Switch and diode utilization factor versus duty cycle of a flyback.

The duty cycle (D) also appears in the transfer function of the flyback converter. If D_{max} is set to 0.5, then the RHPZ of the plant is kept at higher frequencies compared to when the duty cycle is allowed to grow further. Furthermore, a flyback converter with current mode control operating in CCM causes sub-harmonic

oscillation with a duty cycle higher than 0.5. Therefore, the maximum duty cycle is set to $D_{max} = 0.5$ [1].

After determination D_{max} , the maximum voltage experienced by the MOSFET can be calculated by (4.2), where V_{sw} get its maximum value when the input voltage is maximum which corresponds to the minimum duty cycle. The chosen switch should withstand V_{sw} plus the voltage spikes due to the leakage inductance of the transformer, which can be estimated to $0.3V_d$. In addition to this, a 30% safety margin is added [2] which gives the nominal voltage of the MOSFET as

$$V_{ds}^{nom} = 1.3(V_{sw} + V_{spike}) \quad (4.6)$$

where V_{ds}^{nom} is the nominal voltage of the MOSFET.

4.3 Transformers primary inductance (L_m)

A flyback transformer can be modelled as an ideal transformer with a parallel inductor. The inductor should be able to store the energy that the load requires during one period[3][14]. The energy stored in an inductor is

$$W = \frac{1}{2}L_p\Delta i_m^2 \quad (4.7)$$

where W is the energy stored in the core and Δi_m is the ripple current through the inductor as expressed in (3.3). It is expected that the converter should change the operating mode between CCM and DCM as the input voltage and load conditions change. For both operation modes, the critical point occurs at the lowest specified input voltage and full-rated output voltage [1][3]. The inductor should be able to store maximum energy for this point.

One choice to be made is to select the ripple ratio relative to the average on-time current. The average current drawn from the source is

$$I_m = \frac{P_{in}}{V_d D} \quad (4.8)$$

where P_{in} is the input power and I_m and is the average of the magnetising current. The ripple current factor is then defined as

$$K_f = \frac{\Delta i_m}{2I_m}. \quad (4.9)$$

A value of $K_f < 1$ is valid for CCM while $K_f = 1$ means that the converter is operating in DCM. To design a flyback converter operating in CCM, it is recommended to set $K_f = 0.25 - 0.5$ which in this case is set to $K_f = 0.4$. The primary inductance can now be calculated if (3.3), (4.8) and (4.9) are combined to give

$$L_p = \frac{(V_{dmin} D_{max})^2}{2P_{in} f_s K_f}. \quad (4.10)$$

where f_s is the switching frequency. The ripple current can be now calculated from (3.3) and the maximum current that flows through the inductance is

$$I_{peak} = I_m + \frac{\Delta i_m}{2}. \quad (4.11)$$

The RMS value of the primary current is calculated according to the definition of RMS value by applying Simpsons rule as in (4.12). For derivation, see Appendix A.1.

$$I_{rms} = \sqrt{\frac{D}{3} \left[3I_m^2 + \left(\frac{\Delta i_m}{2} \right)^2 \right]} \quad (4.12)$$

Table 4.2: The RMS value of the current and the resulting primary inductance

Frequency [kHz]	I_{peak} [A]	L_{prim} [μ H]	K_f	I_m [A]	I_{rms} [A]	Δi_m [A] (min)	Δi_m [A] (max)
65	4.235	52.5	0.35	3.137	2.263	2.196	2.928
300	=	11.38	=	=	=	=	=

Table 4.2 shows the calculated values for the parameters.

4.4 Core selection

The core selection is an iterative process with trade offs between different properties such as the core geometry (EE, RQ, PQ, EI) the core size and the material of the core (e.g N27 and N87)[12][9][14].

Table 4.3: Core list and design properties

Core List			
Core	Ve [mm^3]	Ae [mm^2]	AP [mm^4]
EE 16/8/5	750	20.1	406
EE 20/10/6	1490	32.1	1120
EE 25/13/7	2990	52.0	3290
EFD 15/8/5	510	15A	240
EFD 20/13/9	1460	31.0	859
EFD25	3300	58	2330
ETD 29/16/10	5350	76.0	7220

Choosing a suitable core shape or geometry is important since different core shapes have different windows area in relation to their sizes. For example, PQ cores have smaller windows area compared to the same size EE core. For a flyback converter it is good to have a wider windows area in order to achieve a lower leakage inductance [16][17]. Therefore, the core chosen was the E family of cores (e.g. EE, EFD, and ETD). Table 4.3 shows some commonly used core sizes and their related data.

Having chosen the core shape, a proper core material should be chosen for the core which is appropriate for the desired switching frequency. The switching frequency is a balance between losses and the transformer's size [9]. As described in section 3.3.1, a high switching frequency leads to higher losses but a markedly smaller transformer size. For high frequency, the eddy currents should be accounted for if the core material has low resistivity. However, with the objective being to show how different switching frequencies can affect the size and efficiency of the converter, two different frequencies are used. A suitable core material for the selected switching frequencies is N87 which can be used for frequencies from 25-500 kHz. The data sheet can be found in Appendix B.1.

In Fig. 4.3, the core per unit volume loss for several B_{ac} values is plotted as function of the switching frequency. The B_{ac} is the peak swing in the flux density around its average. At a given frequency, the core loss density (P_{fe}) can be approximated as

$$P_{fe} = k f_s^\alpha B_{ac}^\beta \quad (4.13)$$

where the exponents α and β and the coefficient k depend on the type of the material.

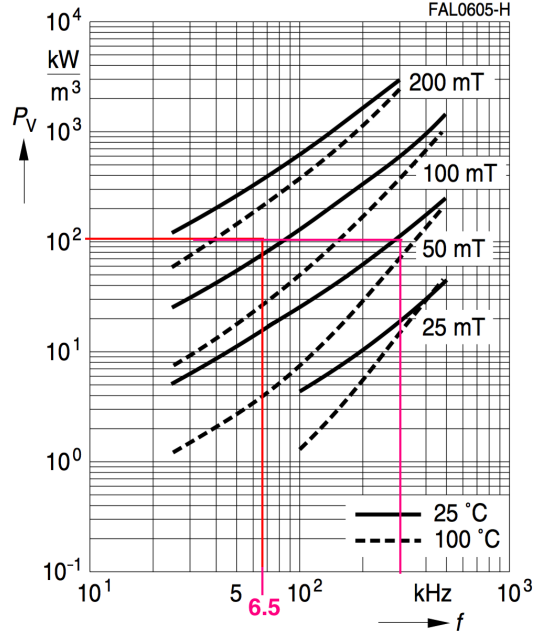


Fig. 4.3: Relative core losses versus frequency for N87 core material

The core size has to be determined as well. Since a flyback transformer is used to store energy, the core size should have sufficient power handling capability while maintaining an acceptable loss. The most commonly used method with many variations, is to use the windows area product (AP) which, as the name suggests, is the product of the effective cross-sectional area of the core and the windows opening available for winding. Manufacturers generally make use of the windows utilisation factor (k_f), the frequency, the transferred power and the maximum flux density as determining factors. However there are significant differences in how the AP is defined and used [14][17].

In general, the limiting factor is either core losses due to the flux density swing ΔB or core saturation. As described in section 3.3.1, B is proportional to H which is in turn proportional to the current. Therefore, the flux swing ΔB is directly related to the ripple current ΔI . For example, it can be seen from Fig 4.4 that a converter operating in CCM will have a relatively low ΔI and consequently a low ΔB . This translates to a low loss value since the area that the hysteresis loop encloses is relatively small as shown in Fig 4.5(a). In this case, the saturation level is the limiting factor for the core utilisation.

On the other hand, if the converter is operating in DCM or BCM, the ripple current is relatively high as seen in Fig 4.4. High ripple current results in high flux swing and the area enclosed by the hysteresis loop becomes larger. In this

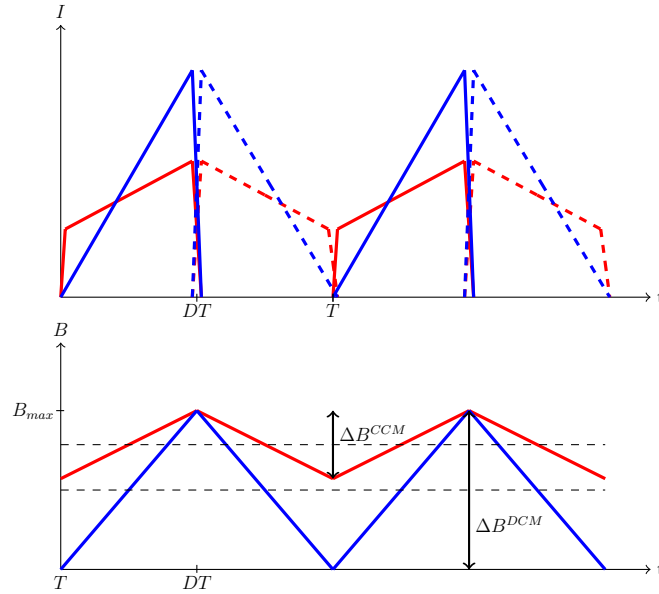


Fig. 4.4: Primary inductor mode current, blue for DCM and red for CCM

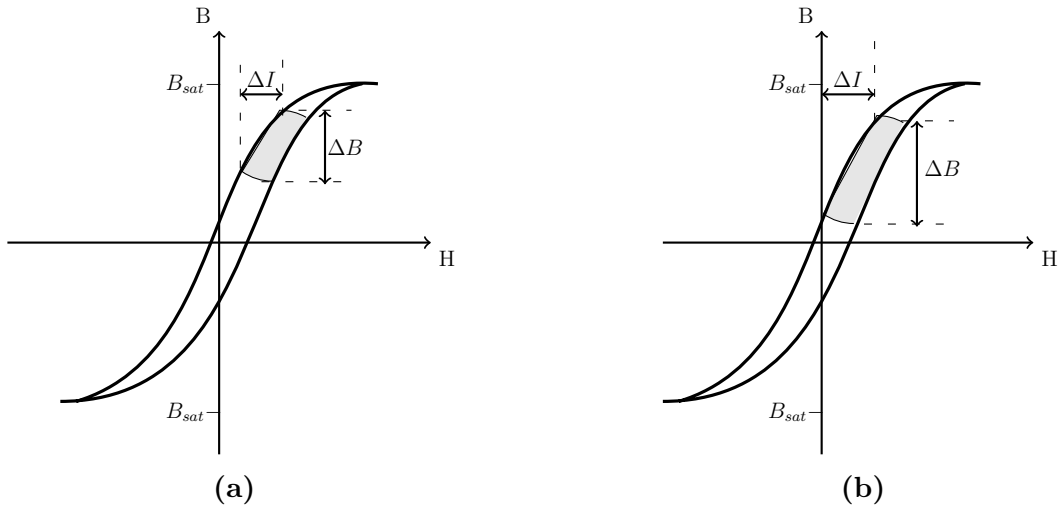


Fig. 4.5: Hysteresis in the B - H plane for ferromagnetic cores. (a) typical flyback operating in CCM. (b) typical flyback operating in DCM

case the limiting factor of the core utilisation will be core losses rather than B_{sat} . Therefore, the ΔB should be limited to a reasonable value to keep core losses acceptable. A reasonable core loss of 100 mW/cm^3 is the maximum for natural convection cooling[16][2].

4.4.1 Determine the maximum flux swing (ΔB_{max})

If the core is B_{sat} limited then the maximum B has to occur 10% above I_{peak} so as to avoid any risk of saturating the core during transients or faults [16][1]. In general, the relationship between ΔI and ΔB can be expressed as

$$\Delta B_{max} = B_{max} \frac{\Delta I_{pp}}{1.1 * I_{peak}} \quad (4.14)$$

where B_{max} is the maximum allowed flux density which usually is less than B_{sat} for practical reasons (in this case set to 300 mT). As can be observed from (3.3), the maximum current ripple occurs at maximum input voltage and minimum duty cycle. For our calculated value ΔI_{pp} of 2.93A, we get $\Delta B_{max}=188.8$ mT. This value is a peak-peak value and it should be divided by two to convert it to the peak value. The core loss per volume due to the peak flux can be found in Fig 4.3. The figure shows that when the switching frequency is 65 kHz the losses are around 100 mW/cm^3 with a peak flux of 100 mT. This means that the core of the converter operating at 65 kHz is saturation limited and B_{max} can be set to 300mT. On the contrary, when the switching frequency is 300 kHz the losses already reach 100 mW/cm^3 when the flux density is barely 50mT. Therefore, the core for 300 kHz is loss limited and the flux swing should not be allowed to exceed $100 \text{ mT} (2 * 50 \text{ mT})$ if it is intended to have low losses [16].

4.4.2 Calculate windows area product AP

When the core is saturation limited, its windows area product can be estimated by

$$AP_{sat} = A_w A_E = \left(\frac{LI_{over} I_{rms}}{B_{max} K_1} \right)^{\frac{4}{3}} \quad (4.15)$$

where L is the primary inductance, I_{rms} is the RMS value of the primary current, and K_1 is a constant ($K_1 = 0.0085$) [16]. As previously discussed, it is safe to set $B_{max} = 300 \text{ mT}$ and the primary inductance, the peak and the RMS current calculated according to (4.10), (4.11) and (4.12) respectively. The core size for the 65 kHz converter can now be estimated to $AP_{sat} = 1306 \text{ mm}^4$. To minimize the number of iterations, it is a good idea to take a core which has a slightly bigger AP. The closest core size of the 65 kHz switching frequency transformer is EFD25.

When the core is loss limited, its area product can be estimated according to

$$AP_{loss} = A_w A_E = \left(\frac{L \Delta I I_{rms}}{\Delta B_{max} K_2} \right)^{\frac{4}{3}} \quad (4.16)$$

where ΔB and ΔI is the maximum flux and current swing respectively. K_2 is a constant ($K_2 = 0.006$). The flux swing should be limited to 100mT which gives an area product of $630mm^4$. For the operating case with a switching frequency of 300kHz, an EFD20 core will be used with $AP = 818mm^4$.

4.4.3 Determine the required number of minimum primary turns N_p^{min}

The minimum number of primary turns N_p^{min} that can provide the desired inductance value when the flux swing is maximum can be calculated as

$$N_p = \frac{\Delta I_{max} L}{\Delta B_{max} A_e} 10^{-2} \quad (4.17)$$

where L is the required inductance and A_e is the cross sectional area of the core. For the converter with the switching frequency of 65kHz, the core is saturation limited and the value of ΔB_{max} calculated from (4.14) is valid. On the other hand, for the converter with the frequency of 300kHz, the core is loss limited at $\Delta B_{max}=100mT$. The value of N_p must be rounded to an integer value.

4.5 Determining the Secondary Turns

The output voltage reflected to the primary side of the transformer when the switch is blocking is given by

$$V_{ro} = \frac{D_{max}}{1 - D_{max}} V_d^{min}. \quad (4.18)$$

A simplified circuit diagram of the transformer is shown in Fig 4.6. The turns ratio of the transformer (n) can be calculated from V_{ro} and the master output voltage V_{o1} which gives

$$n = \frac{N_p}{N_{s1}} = \frac{V_{ro}}{V_{01} + V_{F1}} \quad (4.19)$$

where V_{F1} is the forward voltage drop of diode D_1 (1V) and N_p is specified in (4.17). The number of turns for the second output is calculated from the master output as

$$N_{s2} = \frac{V_{02} + V_{F2}}{V_{01} + V_{F1}} N_{s1} \quad (4.20)$$

where V_{F1} is the voltage drop of diode D_2 . N_{s2} must be rounded to the nearest integer so that the number of the primary turns does not exceed N_p^{min} . The number of turns for the auxiliary is given as

$$N_{aux} = \frac{V_{cc} + V_{Faux}}{V_{01} + V_{F1}} N_{s1} \quad (4.21)$$

where V_{cc} is the nominal voltage of the control circuit and V_{Faux} is the forward voltage drop of the diode D_{aux} . The results are summarized in Table 4.4.

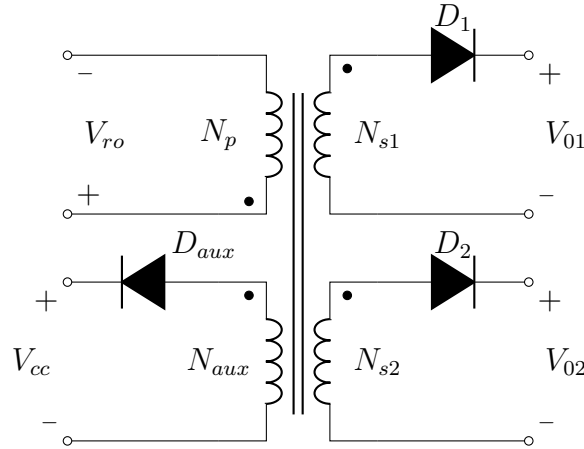


Fig. 4.6: An ideal diagram of the transformer

Table 4.4: Number of turns and core type

Frequency [kHz]	n	N_p	N_{s1}	N_{s2}	N_{aux}	Core type
65	1.4	14	10	5	12	EFD25
300	1.4	11	8	4	9	EFD20

4.6 Determining the Wire Diameter

In order to select a suitable wire size, the RMS value of the current through the primary and the secondary side of the transformer should be known. The selected wire should have enough cross-sectional area so that the temperature increase of the windings becomes sufficiently low. Table 4.5 shows the wire diameter and the current carrying capacity of the wire with different current density. The RMS value of the secondary current can be calculated from the RMS value of the primary current specified in (4.12) which gives

$$I_{sn}^{rms} = I_p^{rms} N K_{ln} \quad (4.22)$$

where K_l is the load occupying factor defined as

$$K_l = \frac{P_{on}}{P_o} \quad (4.23)$$

where P_o is the output power of the selected output. The power of the two outputs is equal and therefore K_l is the same for both outputs.

In order to utilise the cross-sectional area of the wire, a wire of diameter greater than twice the skin depth should be avoided. The skin depth (δ) is defined as the distance from the surface where the current density has fallen by factor of $1/e$ [6]. If the frequency is relatively high, the current density near the surface become very high. The skin depth can be calculated as

$$\delta = \frac{66.2}{\sqrt{f_s}} [mm] \quad (4.24)$$

where f_s is the frequency it is subjected to. The diameter of the wires for the transformer with the switching frequencies 65 kHz and 300 kHz should not be greater than 0.519 mm and 0.241 mm respectively. As seen from Table 4.5, wires with Gauge # 26 and # 31 are suitable for 65 kHz and 300 kHz respectively. A suitable current density in each winding is 395 A/cm^2 . Table 4.6 shows that a number of parallel conductors must be used in order to reduce the skin depth while reducing the AC-resistance. Table 4.5 summarises the results where the design for 65kHz needs 5 parallel wires and the design for 300 kHz needs 15 parallel wires.

Table 4.5: Copper diameter and their current carrying capacity for different A/cm²

Wire List				
Gauge no	Diameter [mm]	Current [A] @329A/cm ²	Current [A] @395A/cm ²	Current [A] @493A/cm ²
25	0.455	0.534	0.6408	0.8010
26	0.404	0.4235	0.5082	0.6353
27	0.361	0.3359	0.403	0.5038
28	0.320	0.2663	0.3196	0.3995
30	0.254	0.1675	0.201	0.2513
31	0.226	0.1328	0.1594	0.1993
32	0.203	0.1053	0.1264	0.1580

Table 4.6: Rms value of the current and the required number of wires

		Number of parallel wires	
Current [A]	RMS value	65 [kHz]	300 [kHz]
I_p	2.263	5	15
I_{s1}	1.5864	4	10
I_{s2}	2.978	6	19

4.7 Choosing the diodes

Proper design of the switch and the diode are essential to any switching converter. The switch has to be dimensioned to be able to withstand stresses while being fast enough. The voltage across the diode when it is blocking is the input voltage transferred to the secondary side of the transformed plus the output voltage according to

$$V_{Dn} = V_{on} + \frac{N_{sn}}{N_p} V_d^{max} \quad (4.25)$$

where V_{Dn} is the voltage across the diode, N_{sn} is the number of secondary turns specified in (4.19) and (4.20) while V_d^{max} is the maximum input voltage. The voltage rating of the selected diode should have at least 30% of safety margin. The nominal voltage of the diode is $1.3V_{Dn}$ [18].

The maximum current that flows through the output diodes is the RMS current of the secondary which is presented in (4.6). The nominal current of the diode should be at least 50% higher than the calculated value [9] to give sufficient margin. Since the master output is designed for 1A, a 1.5A rated diode was chosen and a 3A rated diode for the slave output (design current 2A). They were both available at a rated voltage of 90V which was beyond the requirement.

4.8 Determine the output capacitors

The output capacitors in the flyback converters provide energy to the load during the time that the diode is in blocking mode. See Fig 4.7(a) where the shaded area in the figure represents the charge that flows to the load and is given by

$$\Delta Q = \Delta V_o C_o = DT I_o \quad (4.26)$$

where ΔV_o is the ripple in the output voltage and C_o is the capacitance value. The value of the ripple voltage is dependent on how sensitive the load is to voltage ripple which in this case is set to 0.2% of the output voltage. The minimum capacitor value can be now calculated as

$$C_{min} = \frac{DT I_o}{\Delta V_o f_s} \quad (4.27)$$

where f_s is the switching frequency. As seen from Fig 4.7(b), the current through the capacitor produces a corresponding ripple voltage across the capacitor's equivalent resistance (ESR). The selected capacitor must have an ESR that leads to a lower ripple voltage than ΔV_o . The current rating of the capacitor is given by

$$I_{c(rms)} = \sqrt{I_d^2 - I_o^2} \quad (4.28)$$

where I_d is the RMS value of the current flowing through the diode.

Table 4.7 summarises the chosen ratings of the MOSFET, the diodes and the output capacitors for the designed converters

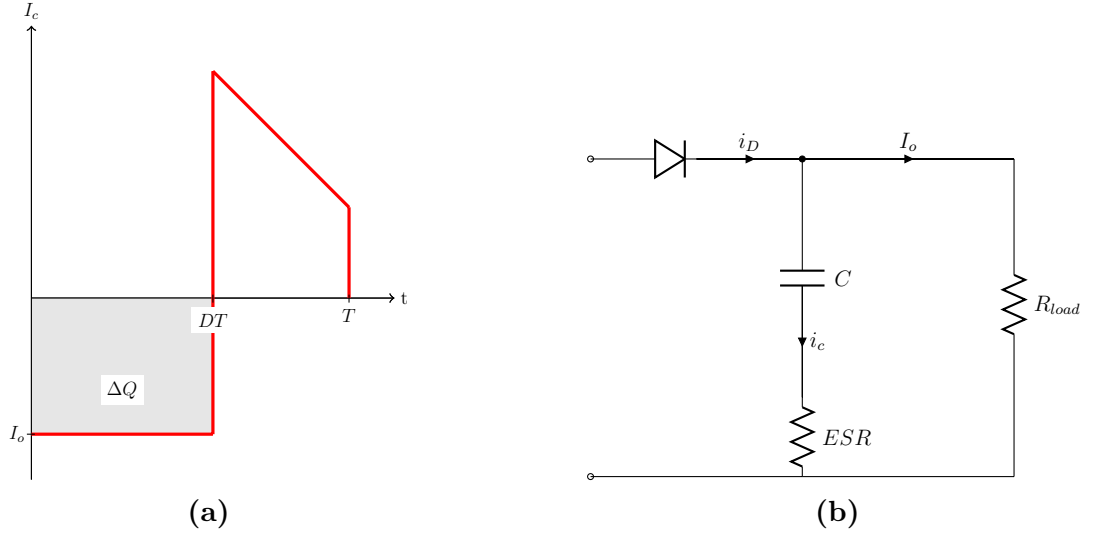


Fig. 4.7: (a) Output capacitor current. (b) Simple circuit diagram of the output capacitor, diode and load

Table 4.7: Ratings of the power stage components

	Power ratings [V/A]			Cap./ESR [$\mu\text{F}/\text{m}\Omega$]	
Frequency [kHz]	MOSFET	D_1	D_2	C_{o1}	C_{o2}
65	70/11	90/1.5	90/3	385	1539
300	70/11	90/1.5	90/3	83	333

4.9 Design of Clamp and Damping circuit

The transformer has a main flux that links the primary with the secondary and leakage flux which causes a leakage inductance. When the switch is off, the lumped capacitance of the switch leads to

$$\frac{dV_D}{dt} = \frac{I_{peak}}{C_{lump}}. \quad (4.29)$$

These spikes have a high rate of change and could exceed the breakdown value of the MOSFET voltage therefore, a clamp circuit is needed to avoid this problem.

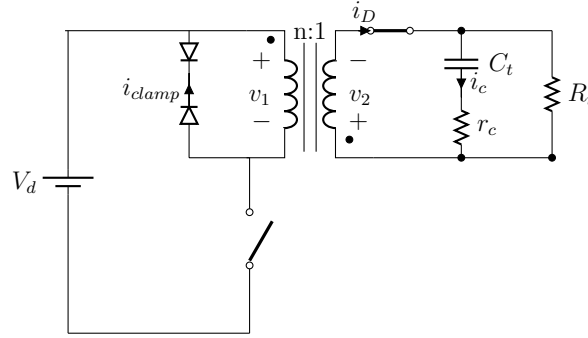


Fig. 4.8: Circuit showing the arrangement of a TVS and diode to achieve clamping

The idea is to connect a low voltage impedance path across the transformer that will conduct once a predetermined voltage level is reached on the drain which is considered safe for the MOSFET. The Fig 4.8 shows such a low impedance path using two diodes. This clamp voltage is set using a Transient Voltage Suppressor (TVS). A safety margin is added to ensure that the switch does not break down. A TVS is simply an avalanche diode that is able to set a clamping voltage based on its avalanche breakdown voltage. It also dissipates the power and thus keeps the drain voltage within acceptable limits. The MOSFET breakdown voltage is 100V and allowing a margin of 30 percent, we can not allow our drain voltage to go beyond 70V. With our maximum input voltage set to 30V, a TVS with an avalanche breakdown of 40V is chosen.

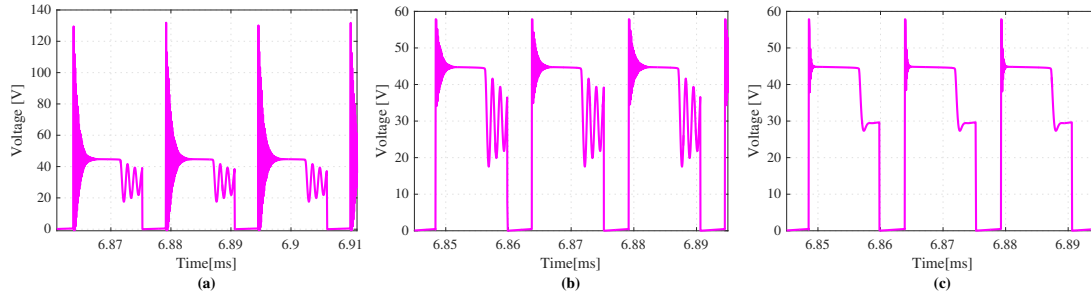


Fig. 4.9: Voltage across the MOSFET: (a) Without clamp (b) With clamp (c) with clamp and damping resistance and capacitor

Fig 4.9 shows the resultant waveforms where the voltage spikes can be seen. This spikes could damage the MOSFET if it was rated for 100V. The solution is to use the designed clamp circuit which then reduces the magnitude of the spikes as shown in (b). A further improvement could be the addition of a damping circuit to reduce the oscillations as shown in (c).

4.10 Compensator Design

The first step in the compensator design procedure is to derive the transfer function of the flyback converter. For the converter shown in Fig 4.10 the state space coefficients are A_1 B_1 C_1 and D_1 for the on-state in Fig 4.10(a), and A_2 B_2 C_2 and D_2 for off-mode in Fig 4.10(b)

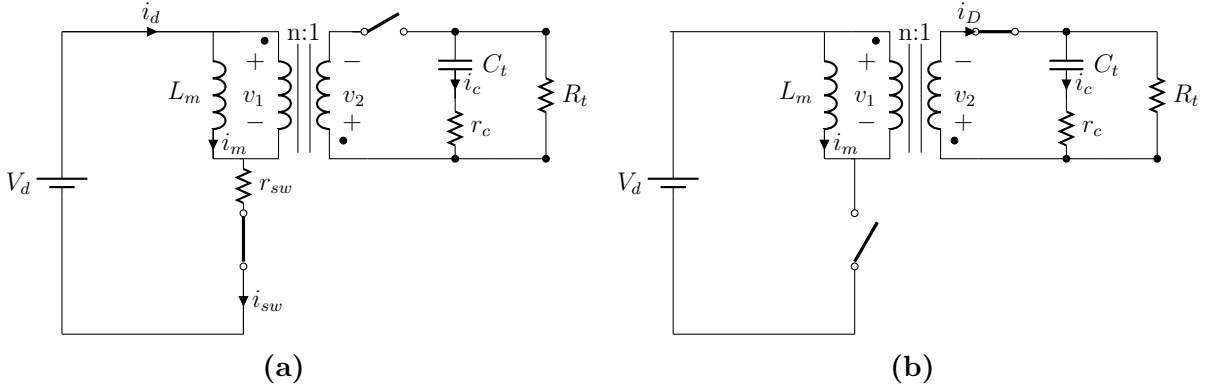


Fig. 4.10: Equivalent circuit of a flyback converter.(a) ON mode (b) OFF mode.

The inductor current, the voltage across the output capacitor and the output voltage give the states of the system. When the switch is on, the inductor current is

$$\frac{di}{dt} = \frac{V_d - i_m R_{sw}}{L_m}, \quad (4.30)$$

while the output voltage is

$$v_o = \frac{R_t}{(R_t + r_c)} \quad (4.31)$$

and the voltage across the capacitor is

$$\frac{dv_c}{dt} = \frac{v_c}{(R_t + r_c)C_t} \quad (4.32)$$

where R_t and C_t are the total load resistance and capacitance respectively. For a converter with more than one output, all the outputs appear in parallel since the inductance current is feeding all of them. Therefore, C_t and R_t are a combination of the load resistance and capacitors of all the outputs [19]. When the switch is conducting the state equations of the system can be written as

$$v_o = \frac{R_t}{R_t + r_c} v_c + \frac{nR_t r_c}{R_t + r_c} i_m \quad (4.33)$$

$$\frac{di}{dt} = -\frac{nR_t}{(R_t + r_c)L_m} v_c - \frac{n^2 R_t r_c}{(R_t + r_c)L_m} i_m \quad (4.34)$$

and

$$\frac{dv_c}{dt} = \frac{nR_t}{(R_t + r_c)C} i_m - \frac{1}{(R_t + r_c)C} v_c \quad (4.35)$$

The resulting state-space equations are presented in Appendix A.2. By averaging the state space matrices, the desired transfer function of the power stage (T_p) can be derived. The derivation of these equation are beyond the scope of this theses but step-by-step explanation has been provided [4]. The small signal transfer function is

$$T_p(s) = C[sI - A]^{-1}[(A_1 - A_2)X + (B_1 + B - 2)V_d] + (C_1 - C_2)X \quad (4.36)$$

where T_p is a function of the duty cycle and the input voltage. The matlab file provided in Appendix A.4 simplifies (4.36) and calculates the compensation parameters (C_1 , C_2 and R_2). The bode diagram of the total system is shown in Fig 4.11 and shows that the system has a zero in the right hand plane when the input voltage at its maximum. This operating point is the most critical point from a controller theory point of view and therefore the compensation parameters are designed at this operating point.

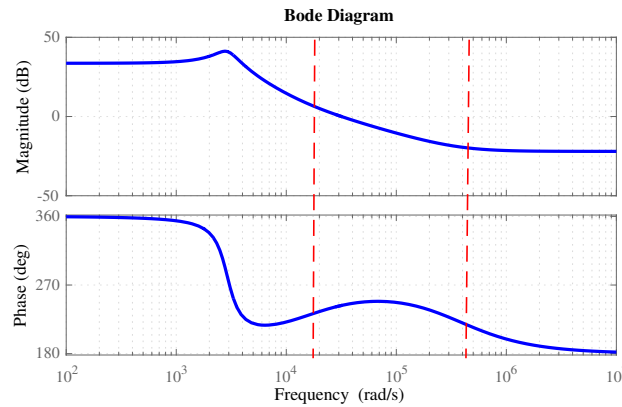


Fig. 4.11: Theoretical bode plot of the system

5

Simulation and PCB Design of a Flyback

5.1 Existing Simulation Model

The existing simulation model is shown in Fig 5.1 where a functional block creates the gate signals to an ideal switch. The students choose a switching frequency and a certain duty cycle (set by voltage V_c) and monitors the change in the output voltage. This simulation is good in showing the basic operating principles but is not reflecting the reality of what a typical control circuit looks like.

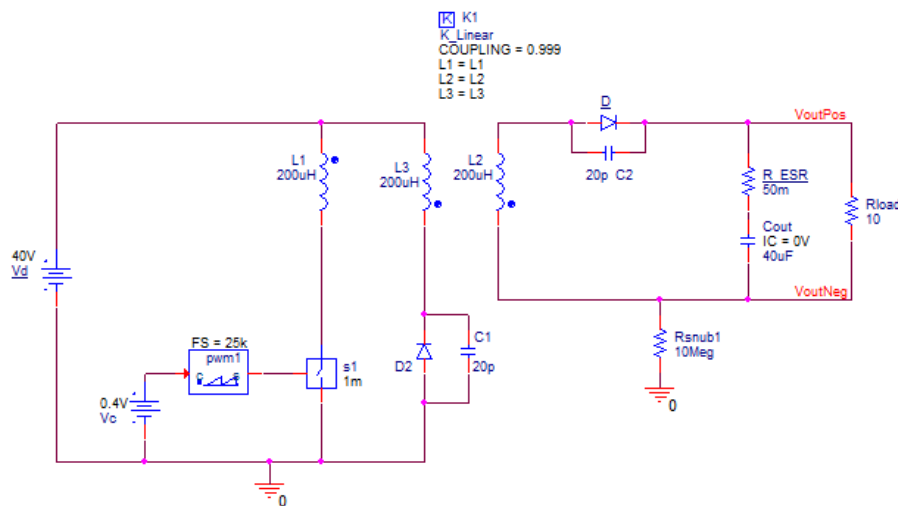


Fig. 5.1: The existing simulation model.

5.2 Proposed Simulation Model

The simulation model of the flyback converter is as shown in Fig.5.2. The simulation was implemented using OrCAD Pspice. The manufacturer of the controller has provided a Spice model that was used in the simulation. A new model of the transformer to enable multiple outputs was developed for this thesis. Below is a description of the different signals and what effect they have on the circuit.

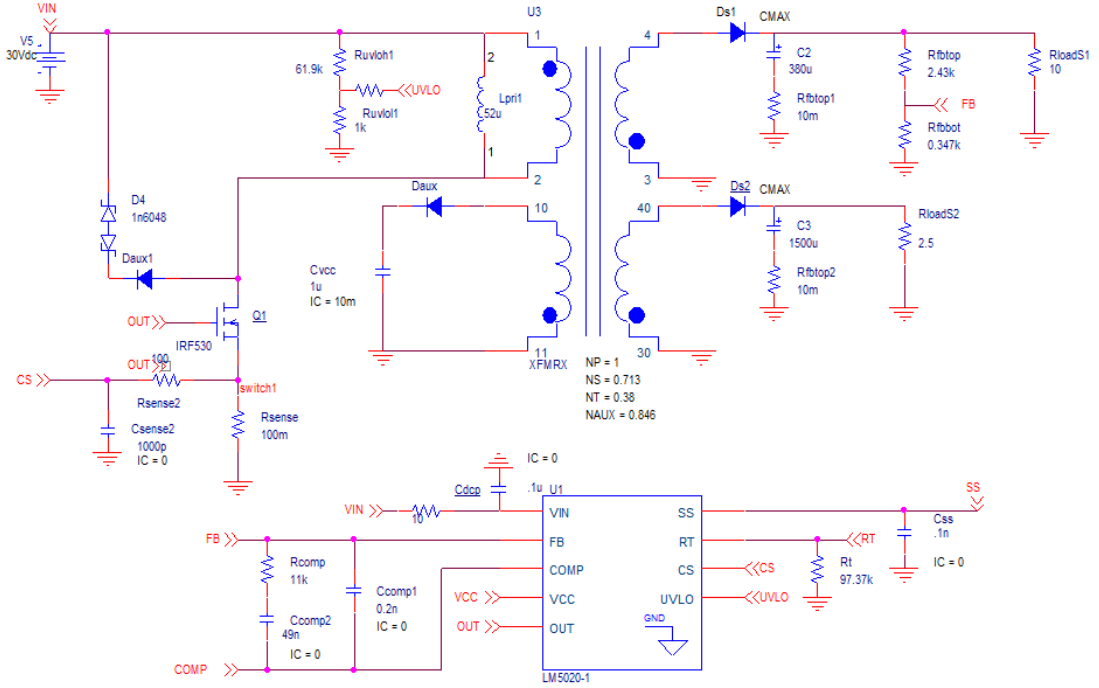


Fig. 5.2: Simulation model of a flyback converter with two outputs

VIN: The LM5020 works on a range of input voltages from 13V to 100V.

UVLO: Signal used to detect an under-voltage in the input and shuts down the controller. The designer chooses what will be the absolute minimum voltage for the circuit to work. Using this value, a voltage divider is used to set this voltage to translate to the UVLO voltage minimum of 1.25V.

VCC: The output to the internal voltage regulator. This voltage is set to 7.7V. An auxiliary winding can be used to set this voltage above that to reduce the power consumption of the chip.

OUT: PWM controller output that drives the gate of the MOSFET with 1A peak current capability.

CS: Current sense pin used for cycle by cycle over-current protection. Any voltage above 0.5V will shut off the controller. A sense resistor in series with the switch is chosen so as to give 0.5 volts when the current threshold is reached.

SS: Soft start pin. A capacitor on this pin sets the gradual ramping of the input to enable the output.

FB and COMP: The compensation network is connected between these two pins.

The new simulation model can be used for transient as well as steady state analysis of the circuit. The effect of having a non ideal switch, transformer, as well as diodes can then give the student a real feel of the actual converter. Students can thus use the simulation for calculation of losses as well as design of snubber circuits for a real life flyback.

Above all, this simulation could be used to show important aspects in control of the flyback and how a proper feedback and compensation network should look like and what effects they have on the circuit. These control aspects can be shown through the step response of the output voltage. An AC analysis was not performed due to lack of time.

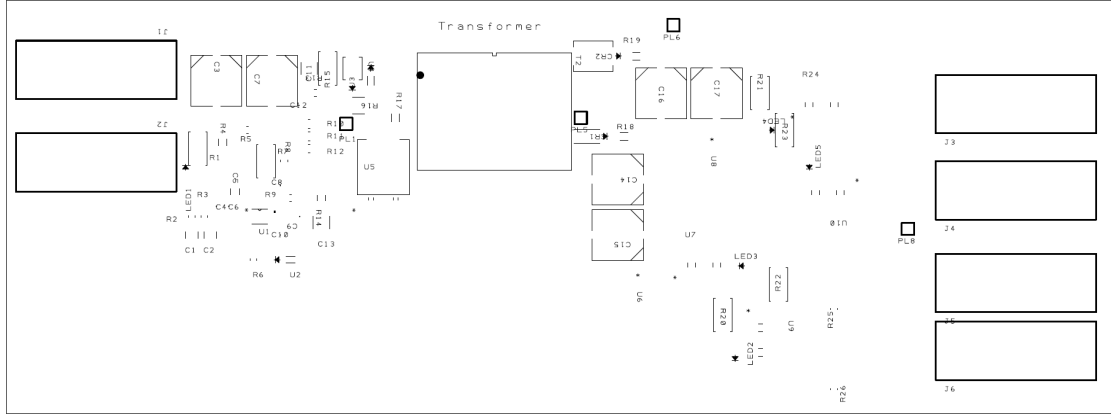
5.3 PCB Design

A Printed Circuit Board (PCB) was designed for the circuit using the free program DesignSpark PCB. The PCB design process is initiated by a working simulation model. The simulation helps in deciding component values that will constitute the final circuit.

The first part of the design involves the creation of build schematics which is composed of how all the components are connected together. Power signals form the main current paths through the input capacitors, the transformer and the switch in the primary side of the converter. For the secondary side its mainly the output diodes, capacitors and the load that have the power nodes. Since a controller is used, it requires some signal nodes as well which are low power traces. Proper grounding is a key factor for the proper functioning of the converter as a whole while power and signal grounds have to be separated.

The following component and trace layout recommendations came in handy in setting up the final PCB board

1. When designing with a current sense resistor, all of the noise sensitive low power ground connections should be connected together locally to the con-

**Fig. 5.3:** Top Silkscreen

troller. A single connection should be made to the high current power ground. This is recommended by the manufacturer.

2. The frequency setting resistor should be located close to the device and connected directly to the pins of the controller
3. The decoupling capacitors on the V_{in} and VCC pins of the controller should be located as close to the controller as possible
4. The power traces from the input voltage and in the output path should be made as thick as possible
5. The current loops that are formed by the input source and the input capacitors, the transformer and the switch should be made as short as possible.
6. The clamp circuit should be located as close to the transformer as possible.
7. If the load is of a resistive nature, it is likely to overheat and therefore the heat is conducted through the PCB. It is therefore recommended to place the load on a separate PCB.

Fig 5.3 and Fig 5.4 show the top silkscreen and copper traces of the final circuit. Fig 5.5 shows the bottom copper layer of the final circuit.

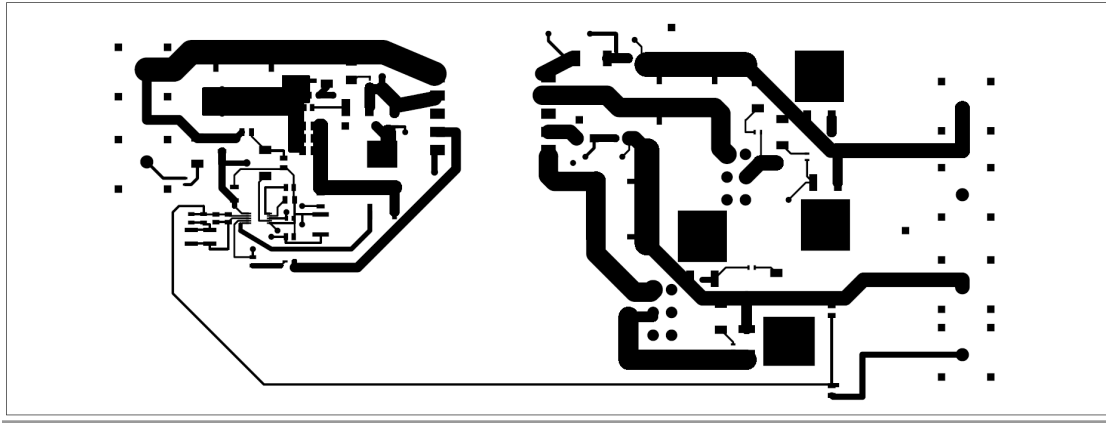


Fig. 5.4: Top copper trace

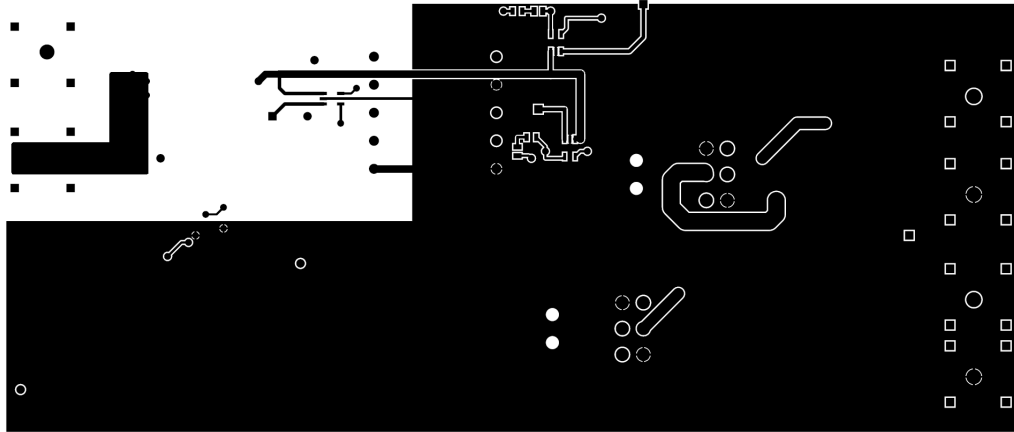


Fig. 5.5: Bottom Copper

5.3.1 Current Measuring

In order to study the operation mode that a flyback converter is operating, the waveforms of the current and the voltage should be measured. The voltage and the currents that are important to measure is shown in Fig. 3.4, 3.3 and 3.5. There are different ways that can be measured the current. One of these methods is to use a current sense amplifier. This device measures a voltage drop over a sense resistor placed at the path of the current. For example, the current through the switch can be measured by serially connecting a $100\text{ m}\Omega$. The current sense amplifier used in this thesis is MAX4173 which has a gain of $+100\text{V/V}$ and wide 1.7MHz bandwidth.

6

Simulations and Measurements

6.1 Simulations

The simulation model and the practical lab assignments should be connected to the theoretical aspects of the converter as explained in chapter 3. The simulation model developed in this thesis is a simple model of a flyback converter in which transformer of the flyback is modelled as an ideal transformer in parallel with a magnetising inductance. The model is intended to demonstrate the operating principle of a flyback converter by demonstrating the different operation points (CCM and DCM) and what causes the transitions between them. Some of the parameters are summarised in (3.15) and shown in Fig. 3.6. Unlike the existing simulation model, this model simulates a closed loop system of a flyback converter.

6.1.1 Inductance value in CCM

The students can calculate the minimum value of the magnetising inductance L_m which give CCM as home assignment. The value of the magnetising inductance used in this project is calculated from (4.10) and Fig. 6.1 shows how the waveforms changes when the input voltage increases. This is aligned to the mathematical equations demonstrated in Fig. 3.6 which show that the duty cycle decreases as the input voltage increases. This means that the time that the transformer is discharging increases relative to the charging time and explains the transition to DCM. Students can verify and investigate some of the mathematical relationship explained in chapter 3 by studying Fig. 6.1. For example, the students can investigate:

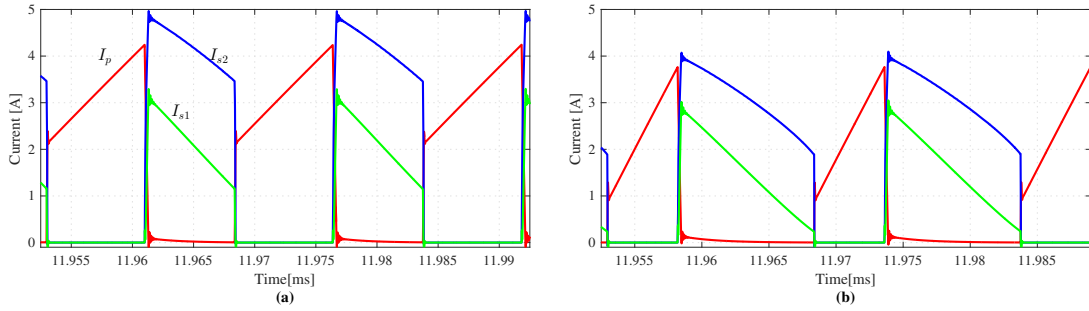


Fig. 6.1: Simulation: Current waveforms in a flyback converter operating in CCM mode with different input voltages: (a) $V_d=15$ (b) $V_d=30$.

- The input voltage that gives the maximum and minimum ripple currents.
- The ripple current that gives the maximum core losses. The core losses can not be measured in the simulation but theoretically a high current ripple results a high magnetic flux swing which in turn gives a high core losses.
- The input voltage that leads to the maximum duty cycle.

If the load is decreased, the system shifts to discontinuous conduction mode. The duty cycle continues to decrease as the output current decreases. Fig 6.2 shows that when the output voltage is maximum and the output current is minimum the system is operating in DCM. As the input voltage decreases the system shifts to CCM. This phenomena is also illustrated Fig.3.6. Load changes therefore affect the operation mode in direct response to the energy required to be transferred to the output. The shift between different modes can thus be achieved by changing the load current or input voltage. The pedagogical tasks that the students can investigate from this are:

- When ever the input or output voltages change the resulting automatic change in the duty cycle will be an interesting demonstration to the students.
- The system can shift to DCM if the load current decreases

6.1.2 Inductance value in DCM

The transformers magnetising inductance is a critical parameter that determines the operation mode. A high primary inductance L_m means that more energy can be stored in the transformer every cycle and it is very likely that this energy will not be dissipated in the same cycle, the converter will thus operate in CCM.

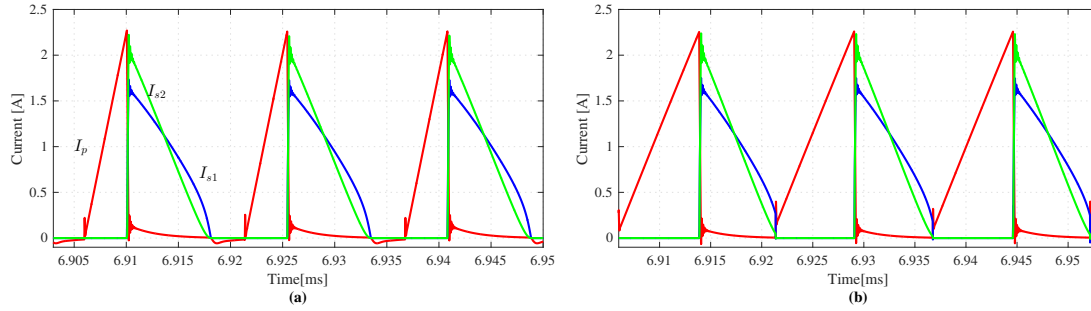


Fig. 6.2: Current waveforms in a flyback converter operating in DCM mode with different input voltages: (a) $V_d=30$ (b) $V_d=15$.

Lowering the inductance value will change the operation mode of the converter. This phenomena is presented in Fig. 3.6 which shows that a low inductance value is needed in DCM. In the designed circuit, the operation point is changed by replacing the core with another that has a bigger air gap thus decreasing the inductance value and consequently changed the operation mode. A change of inductance from $52.5\mu\text{H}$ to $18\mu\text{H}$ for the same input and output conditions led to change from CCM to DCM operation. The pedagogical tasks that the students can analyze are:

- The inductance value needed in DCM is less than one in CCM. Therefore, the size of the transformer can be reduced when operating DCM. This tasks demonstrates that the transformer of a flyback converter is an energy storage device and the size of it is directly proportional to the stored energy.
- As can be observed from Fig. 6.2 and Fig. 6.3, the ripple and peak current are relatively high in DCM compare to CCM. This leads to high losses in the MOSFET and the diode. Therefore, it is preferred to use DCM for the low current high voltage applications.

6.1.3 Current sense simulations

To measure the current through the switch and the diodes, a current sense amplifier was implemented. The amplifier should have a relatively high bandwidth in order to measure the high frequency content of the current. Fig. 6.4 shows the simulation result where the actual value of the current is compared to the current sense results.

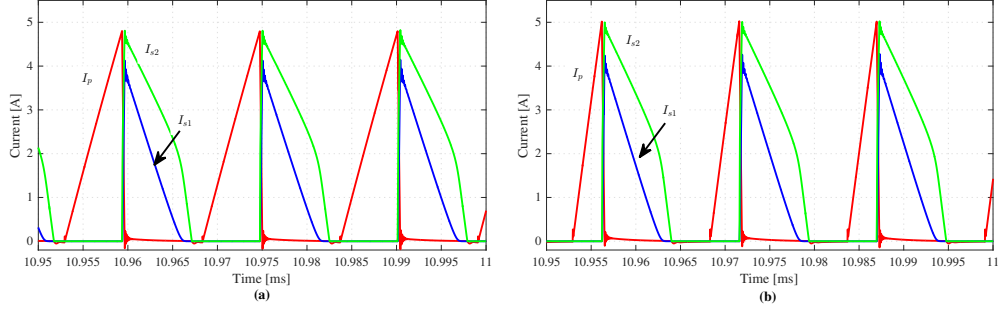


Fig. 6.3: Simulation: Current waveforms in a flyback converter operating in DCM mode with different input voltages: (a) $V_d=15$ (b) $V_d=30$.

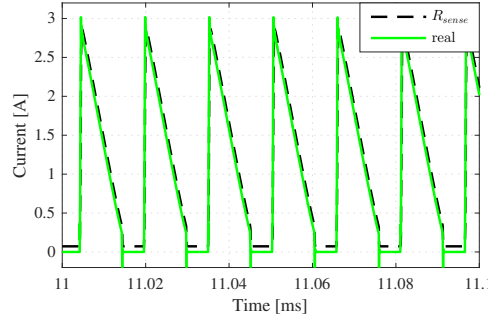


Fig. 6.4: Current measurement in the simulation model

6.1.4 Compensation Network

One problem for this simulation model is the compensation network which should be tailored to the transfer function of the power stage. When the inductance value or the frequency is changed, the parameters of the compensation network should be recalculated which can be difficult to the students. This problem can be solved by preparing the compensation network parameters to the students. For example, the Matlab file provided in Appendix A.4 calculates the compensation parameters according to the course literature in [4]. The matlab function takes the frequency and inductance value as input arguments. And printouts the values of the compensation network. Fig.6.5 shows the step response of the system when a step was applied to the master output. As seen from Fig 6.5(a), the controller reacts to bring the voltage back under control. The design of the compensation network will be done for a particular operation mode which makes transitions between the different operating modes particularly prone to stability issues.

On the other hand, when a step is applied on the second output (the slave output)

the voltage decreases as it can be observed from Fig. 6.5. An understanding of this concept will help the students to appreciate the role that the controller plays in stabilizing the output voltage in a flyback converter.

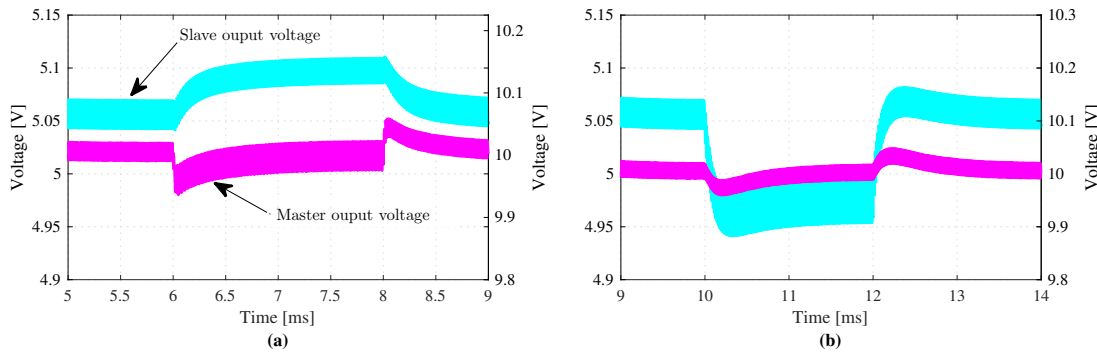


Fig. 6.5: Transient response of the output voltage: (a) When load-step is applied at input 1 (b) When load-step applied at input 2

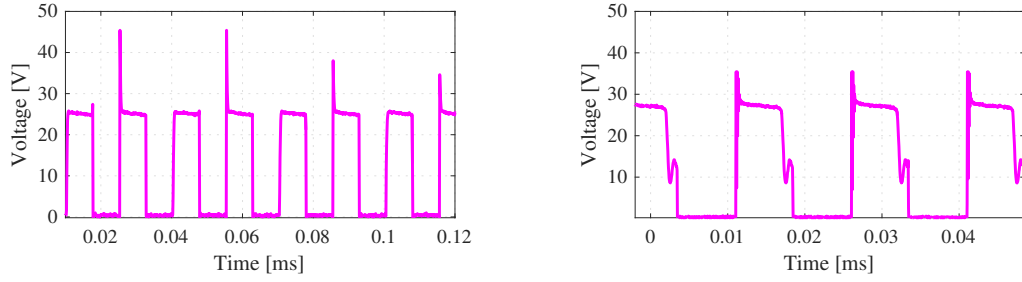
6.2 Measurements

One of the main aims set out in this masters thesis is to make an immediate correlation between the lectures and the lab exercises. The areas of study for the prototype of the circuit board are the current and voltage waveforms.

To achieve these aims, it should be possible to measure currents and voltages in the circuit board so as to see the waveforms. The currents of interest are mainly those through the switch and diodes. The current through the output capacitors could also be shown. The voltages over the switch, the diode and the output voltage would be of interest for the objectives of the course. However, when the current sense is implemented on the circuit board the result it gives is not as expected. This could be attributed to low bandwidth as well as interference due to non optimal placement of the current sense amplifiers. Therefore, to show the operation of the converter, the functionality is illustrated with the voltage across the switch.

Fig 6.6a shows the drain voltage for CCM operation for high output current. This circuit was designed with two different load values that one can switch between. One of the loads is a high resistance load which translates to low current while the other load point is a low resistance load.

A modification was made in that the load was switched to the high resistance load



(a) Drain Voltage when the load current is maximum (b) Drain Voltage when the converter is lightly loaded

Fig. 6.6: Measured result

thus reducing the output current. Fig 6.6b shows the resulting drain voltage. It can be seen that the operation point has changed to DCM.

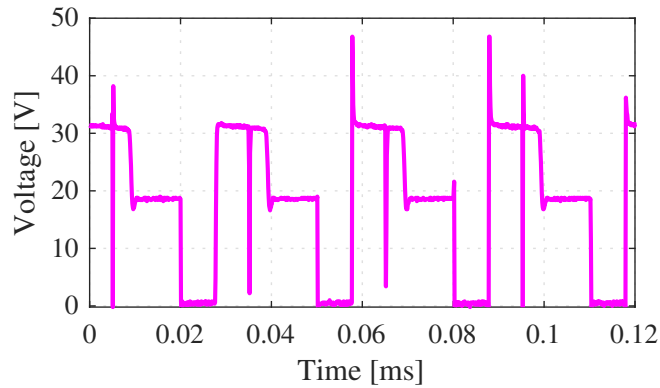


Fig. 6.7: Drain Voltage with lower inductance value

A further modification is done which involves replacing one half of the E-core with one that has a bigger gap effectively reducing the inductance value of the transformer. Fig 6.7 shows the resulting waveforms. Not only has the operation point gone deeper into DCM but there is evidence that the controller is not stable and sends gate signals to the MOSFET when it is in blocking mode. This as discussed earlier is one of the effects related to the compensation which was designed for CCM in this case.

7

Results

From pedagogical point of view, the suggested simulation model and the circuit board upgrades the lab sessions of the flyback converter as follows:

1. One of the main aims set out in this masters thesis is to make an immediate correlation between the lectures and the lab exercises. This is achieved by a simple circuit as shown in Fig. 7.1. The figure shows the different parts of the schematic of a flyback and the corresponding parts of the circuit board.

The suggested areas of study for this circuit board are as follows:

- Load current: Change the load current by switching on two different loads to observe the effect on the circuit waveforms.
 - Inductance: Investigate the effect of changing the transformer inductance on the circuit waveforms. This can be achieved by changing the air gap. The advantage of this task is that it give students a practical understanding how the air gap and inductance value are related.
 - Compensation: Investigate the compensation network and its effect on the stability of the output especially during transitions from CCM to DCM and vice versa. The circuit board that uses in the lab today is open loop system and can not demonstrated the stability issue when the system shifts from CCM to DCM.
2. In order to investigate, the relation between frequency and the size of the transformer, two transformers adopted for two frequencies (65 kHz and 300 kHz) are designed. Fig. 7.2 shows the overview of the two transformers, the volume of the transformer with 65 kHz is 1490 mm^3 and 3300 mm^3 for the transformer with 300 kHz. The size of the transformer decreases with

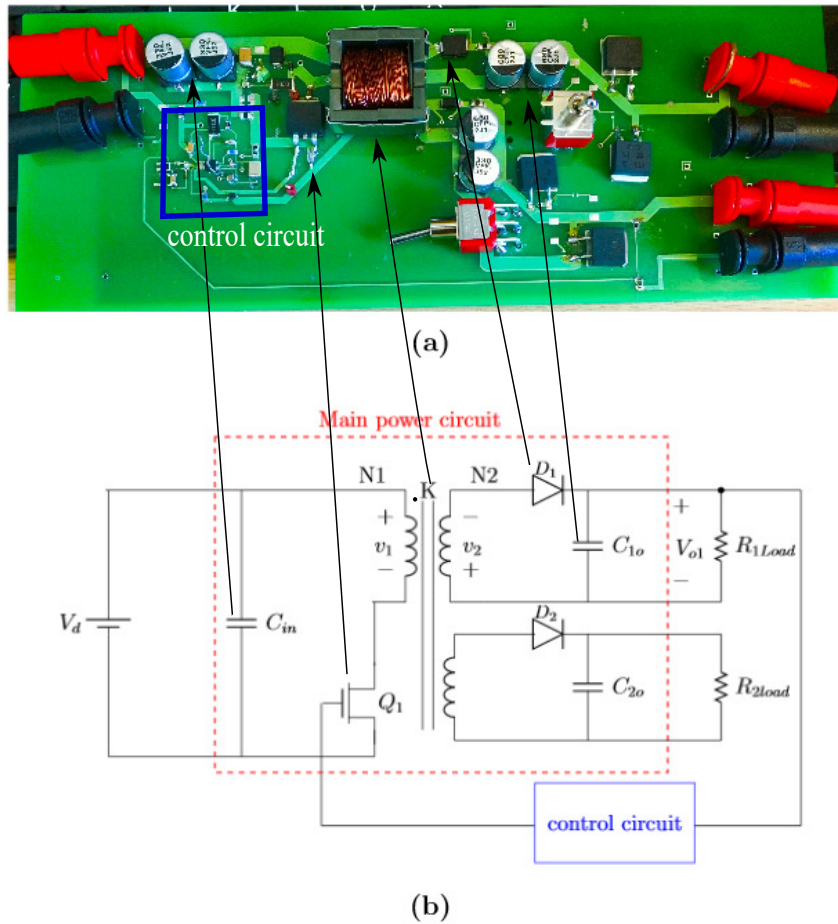


Fig. 7.1: Overview of the circuit board compared to the circuit diagram of the flyback converter.

a factor of 2 although the frequency is increases a factor of 4. This is due to the fact that the flux swing of 65 kHz and 300 kHz are 50 mT and 100 mT, respectively. A suitable pedagogical task that can demonstrate how the frequencies affect the physical size and losses in the magnetic cores is essential. If the two converter are build the only thing that the students can study is the losses and compare the efficiency of the two converters. However, this is not showing much about the magnetic flux in the magnetic cores. Therefore, this thesis is suggesting that the 65 kHz circuit should be build and use it to demonstrate practical lab assignments. Then a suitable pedagogical tasks is redesigning of the transformer, from a frequency of 65 kHz to a frequency of 300 kHz. Due to the practical reasons, the students

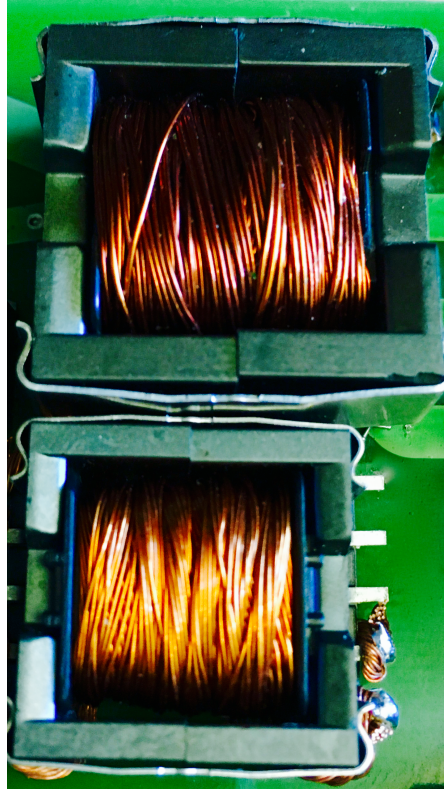


Fig. 7.2: Overview of two transformer with two different frequencies. The frequency of the large and small transformers are 65 and 300 kHz respectively

can, design a transformer with frequency of 300 kHz. The important thing is that the students gets the knowledge of how to design a transformer and understand the basic properties such as the difference between when the core is loss or saturation limited.

3. Demonstration of how the inductance value can change the operation mode of the converter.
 - In the simulation this can be done by theoretically calculating the inductance value which gives CCM and it can be compared to the inductance value which gives DCM. The simulation model verifies if the calculated inductor value behaves as it is supposed to. This tasks demonstrates the function of a flyback transformer which is an energy storage device. The amount of energy needed to be stored for the two operation modes (CCM and DCM) are different, therefore their inductance value are different.
 - In the practical lab, the inductance value can be varied by changing

the air gap. This task can give students a practical understanding how the air gap and inductance value are related. The core used in this project has form of EE and has the gap between the two E. As it can be observed from Fig. 7.2, it can be removed one of the cores and changed to it with one which have larger or smaller gap.

4. Demonstration of how a flyback converter designed to operate in CCM can shift to DCM. This phenomena is explained and discusses in section 3.2.3. The operation mode can be changed by changing the load or the input voltage. In the existing simulation and practical lab it can not be demonstrated what could happen for instance when the input voltage changes. The new simulation model is a closed loop system and the duty cycle changes automatically when the input voltage changes. Therefore, the students can study how the duty cycle changes when the input voltage varies.
5. The flyback converter designed in this masters thesis has two outputs and the controller regulates just one output. The reaction of the controller can be investigated by applying a load step. This task demonstrates that a flyback converter may have two or more outputs but only one output can be regulated.

8

Discussion

The purpose of this thesis was to develop a simulation model and a circuit board for a flyback converter to be used by students of power electronic converters. The designed model is used to visualise the operating principle of the flyback converter. The focus was on three main areas; different operations modes of the converter, transformer design and the role of the controller in the overall function of the converter.

First the different operation modes of the converter is really at the heart of what the student should understand in the course. Terminology such as DCM and CCM mode of operation are a constant presence in ENM060 and ENM070. However, beyond identifying the different waveforms, it is not usually appreciated why a particular operating mode is advantageous or what it means for the converter. Examples are when a certain operation mode is preferred over another with regards to the output voltage and current, the stresses experienced by the switches and diodes and sometimes why a particular operation mode is easier to stabilize than the other.

Secondly, for the flyback converter, the transformer plays an important role as an energy storage element. Even though the design of a truly optimised transformer may be a daunting task with many considerations, a general feel for how to make design choices may be a desirable outcome of future lab work. Principles such as the effect that the switching frequency has on the size of the transformer, the role of the air-gap, and the saturation effects are of importance to the student. Two different transformers were designed for 65kHz and 300kHz and the results show that it is not really a scaling factor that is applicable for the two different frequencies. The inductance value will grow proportionally but this is not true for the physical size as well. The magnetic flux swing allowed for 65kHz

is double that for 300kHz (in the range of 200mT) which leads to different core utilization.

Finally, the controller ensures proper functionality of the converter but is often sidelined in the current course material and its function replaced by PWM generation blocks. It has become clear that a thorough understanding of the controller is essential for the student. Although it may not be necessarily detailed knowledge that is the aim here, at the very least an understanding of how to choose the right controller is beneficial. Feedback design and compensation is key to proper functioning of the converter. Other functions of the controller such as over-current protection and undervoltage lockout (UVLO) could be introduced to the students.

To verify that it is possible to introduce the student to the concepts discussed above, two tasks were undertaken as initial work towards improving the existing lab. A simulation model based on an actual controller and a model of the transformer was built. A PCB prototype was also designed and built and measurements made to verify that it is possible to show the concepts to the students. It is proposed that building the circuit to have as few components as possible and having a layout that is close to what the students are used to seeing in schematics will be of immense benefit to the learning process. However, the current sense amplifier did not work as it suppose to. Measuring of the current through the switch and the diodes are very important and students should be able to measure it. The current sense amplifier is simulated before it was implemented and the result shows that the amplifier has enough bandwidth to measure the current. However, in the practical lab the result that the current sense amplifier gives is not correct. This can be due to one or several reasons combined together. The current sense is placed near the transformer and there is a chance that the leakage inductance can cause a high di/dt which can effect the performance of the current sense. Another problem is that the current sense is not placed close enough to the sense resistor which makes the system vulnerable to the disturbances from the other devices. However, the exact reason that the current sense did not work was investigated due to the lack of time.

9

Conclusion and Future Work

9.1 Conclusion

Power electronics is an important area that has numerous applications and is rapidly expanding. A good base knowledge is essential for students in the masters program in Electric Power Engineering. This thesis has investigated the existing lab and suggested areas where it could be necessary to put a bit more focus by enhancing subjects taught in the lectures with practical lab work. It is clear that emphasis should be placed on the different operation modes; when and why they are applicable and what design choices have to be made to attain such a converter.

A simulation model for a two output converter was created and a prototype PCB board built based on this. The designed simulation and prototype board has few components which makes it possible for their use as supplementary materials in the courses. Three main areas came out as focus points for this thesis; a thorough understanding of modes of operations, magnetics design and controller design. These three areas should form a good basis for lab work in these courses.

A major suggestion of this work is that a design project should be created to simulate and build a DC/DC converter. To fit within the allocated time, the students should have a ready PCB board but they should then focus on choosing the right components and designing a flyback transformer.

9.2 Future Work

There are a few areas that require further work and analysis. Below are some few of the most important.

- Isolation: The designed feedback loop is a non isolated. However, it is quite common that modern flyback converters are isolated using an opto coupler network. This would form an excellent task in improving our flyback design.
- Current Measurement: A current sense amplifier was used to try and visualize the current through the switch and diodes. However the results were not as expected. This was attributed to the bandwidth of the amplifier IC which was probably not sufficient. Different amplifier components were seen to give better results in the simulations which should be investigated further.
- Load: The load was made of power resistors which got quite hot if the converter was operated for longer periods. Further work in this area could be suggestion of different types of loads or even designing of heat sinks.
- Compensation: As discussed in the results, instability was observed in the measurements during transition from CCM to DCM. Further analysis on the compensation network for the flyback converter is therefore necessary.
- PCB Design: There are various improvements that could be made on the compactness as well as other aspects of the PCB.

Bibliography

- [1] FairChild Semiconductor, Design Guidelines for Off-line flyback converter Using Fairchild Power Switch (FPS), rev.1.0.3 (1 2003).
- [2] A. I. Pressman, K. H. Billings, T. Morey, A. (e-book collection), Switching power supply design, 3rd Edition, McGraw-Hill, New York, 2009.
- [3] M. Brown, S. A. (e-book collection), S. (e-book collection), Practical switching power supply design, Academic Press, San Diego, 1990;2012;.
- [4] N. Mohan, T. M. Undeland, W. P. Robbins, Power electronics: converters, applications and design, 3rd Edition, Wiley, Hoboken, N.J, 2003.
- [5] M. K. Kazimierczuk, Pulse-width modulated DC-DC power converters, Wiley, Chichester, U.K, 2008.
- [6] S. Maniktala, S. (e-book collection), B. (e-book collection), Switching power supplies A to Z, second;2nd;2; Edition, Elsevier/Newnes, Amsterdam, 2012;2014;.
- [7] S. Maniktala, S. (e-book collection), B. (e-book collection), K. (e-book collection), E. (e-book collection), I. Books24x7, Troubleshooting switching power converters: a hands-on guide, Elsevier/Newnes, Amsterdam;Boston;, 2008;2011;2007;2014;.
- [8] N. Coruh, S. Urgun, T. Erfidan, Design and implementation of flyback converters, 2010, pp. 1189–1193.
- [9] Infineon Technologies North America, Design Guide for Off-line Fixed Frequency DCM Flyback Converter, design Note DN 2013-01 (1 2013).
- [10] C. W. T. McLyman, Transformer and inductor design handbook, 3rd Edition, Vol. 121., Dekker, New York, 2004.

- [11] D. K. Cheng, Field and wave electromagnetics, 2nd Edition, Addison-Wesley Pub. Co, Reading, Mass, 1989.
- [12] R. W. Erickson, D. Maksimovic, S. A. (e-book collection), Fundamentals of Power Electronics, 2nd Edition, Springer, New York, 2012.
- [13] W. G. Hurley, W. H. Wölflé, B. (e-book collection), E. (e-book collection), I. Books24x7, Transformers and inductors for power electronics: theory, design and applications, 1st Edition, Wiley-Blackwell, Chichester, West Sussex, 2013.
- [14] STMicroelectronics, OFFLINE FLYBACK CONVERTERS DESIGN METHODOLOGY WITH THE L6590 FAMILY, rev.1 (5 2001).
- [15] C. P. Basso, A. (e-book collection), Switch-mode power supplies: SPICE simulations and practical designs, McGraw-Hill, New York, 2008.
- [16] Texas Instruments Incorporated, Inductor and flyback Transformer Design, section 5 (5 2001).
- [17] Texas Instruments Incorporated, Power Transformer Design, section 4 (1 2011).
- [18] D. Z. Chen, B. D. Bai, Multiple output single-ended flyback dc-dc switching power supply design, Applied Mechanics and Materials 392 (2013) 494.
- [19] H. Choi, Practical feedback loop design considerations for switched mode power supplies.

A

Derivations of the mathematical equations

A.1 Converter

The RMS value of the current is defined as:

$$I_{rms} = \sqrt{\frac{1}{T} \int_0^T i(t)^2 dt} \quad (\text{A.1})$$

The definition for Simpsons rule is:

$$\frac{1}{T} \int_{t_o}^{t_o+T} f(x) dx = \frac{1}{6} (f(t_o) + 4f(t_o + \frac{T}{2}) + f(t_o + T)) \quad (\text{A.2})$$

The RMS current of the primary inductance operating in CCM can be calculated as:

$$\begin{aligned}
I_{rms} &= \sqrt{D \frac{1}{DT} \int_0^{DT} i_m dt} \\
&= \sqrt{\frac{D}{6} \left[\left(I_m - \left(\frac{\Delta i_m}{2} \right) \right)^2 + (4I_m)^2 + \left(I_m + \left(\frac{\Delta i_m}{2} \right) \right)^2 \right]} \\
&= \sqrt{\frac{D}{6} \left[6I_m^2 + 2 \left(\frac{\Delta i_m}{2} \right)^2 \right]} \\
&= \sqrt{\frac{D}{3} \left[3I_m^2 + \left(\frac{\Delta i_m}{2} \right)^2 \right]}
\end{aligned} \tag{A.3}$$

A.2 Control

On-mode state-space

$$\begin{aligned}
A_1 &= \begin{pmatrix} \frac{r_{sw}}{L_m} & 0 \\ 0 & \frac{1}{(R_t + r_c)} \end{pmatrix} & B_1 &= \begin{pmatrix} \frac{1}{L_m} \\ 0 \end{pmatrix} & C_1 &= \begin{pmatrix} 0 & \frac{R_t}{R_t + r_c} \end{pmatrix} \\
A_2 &= \begin{pmatrix} \frac{n^2 R_t r_c}{L_m (R_t + r_c)} & \frac{-n R_t}{L_m (R_t + r_c)} \\ \frac{n R_t}{C_t (R_t + r_c)} & \frac{-1}{(R_t + r_c)} \end{pmatrix}, & B_2 &= \begin{pmatrix} 0 \\ 0 \end{pmatrix} & C_2 &= \begin{pmatrix} \frac{n R_t r_c}{R_t + r_c} & \frac{R_t}{R_t + r_c} \end{pmatrix}
\end{aligned}$$

and state average is

$$A = A_1 D + A_2 (1-D)$$

$$B = B_1 D + B_2 (1-D)$$

$$C = C_1 D + C_2 (1-D)$$

where D is duty cycle

A.3 Filter

A.4 Matlab code for compensation network

```

function [R1,C1,C2] = compen(fsw,Lm)

s = tf('s');

% *****
% Component constants
% *****

Vo1=10;
Io1=1;

Vo2=5;
Io2=2;

Rl1=10;
Rl2=2.5;
% the output load is the total load
Rload=(Rl1*Rl2)/(Rl1+Rl2);

% Input voltage, turn ratio and switching fequancy
Vd=30;
Dmin=0.333;
Dmax=0.5;
fs=fsw*1e3;
n1=1.4;
RT1=(1/(fs*158e-12))*1e-3;

% Magnetising inductance;
Lm=Lm*1e-6;

% Calculation of Output capcitors

Voutrps=0.002*10; % ripple voltage houtput 1
Voutrpt=0.002*5;% ripple voltage output 2

Co1=((Io1*Dmax)/(fs*Voutrps));

```

```

Co2=((Io2*Dmax)/(fs*Voutrpt));

Cout=(Co1+Co2); % the total cap. is Cout1//Cout2
rc=30e-3;          % ESR
rsw=70e-3;         %DCR

% Peak value of sawtooth wave
Vtri = 10;

%*****
% States of the power stage: x'=Ax+Bu; y=Cx+Du **
%*****

a211=(n1^2*Rload*rc)/(Lm*(Rload+rc));
a212=(n1*Rload)/(Lm*(Rload+rc));
a221=(n1*Rload)/(Cout*(Rload+rc));
a222=1/((Rload+rc)*Cout);

A1=[-rsw/Lm, 0; 0, 1/((Rload+rc)*Cout)];

A2=[-a211, -a212; a221, -a222];

B1=[1/Lm; 0];
B2=[0; 0];

C11=[0, Rload/(Rload+rc)];
C22=[(Rload*rc*n1)/(Rload+rc), Rload/(Rload+rc)];

A=A1*Dmin+A2*(1-Dmin);
B=B1*Dmin;
C=C11*Dmin+C22*(1-Dmin);
X=inv(A)*-B*Vd;
f=((A1-A2)*X+(B1-B2)*Vd);

%*****
%% Transfer function of power stage %%
%*****

```

```

Tp=simplify (C*inv (s*eye(2)-A)*f+(C11-C22)*X);
%bode(Tp):
[z,p,k] = zpkdata(Tp, 'v');
wz1=abs(real(min(z(2))));
wz2=abs(real(max(z)));
wp1=abs(real(min(p)));

Tm = 1/Vtri;
%% From matlab file used in the ENM060 course written
%%by Massimo Bongiorno and Andreas Karvonen, November 2007
% Add the modulator and the power-stage together
T_converter = Tp*Tm;
% %*****
% % Design of regulator
% % *****
%
% % Desired crossover frequency
% % Should be at least a tenth of the switching frequency
wcross = 0.06*fs*2*pi; %To be changed during the laboration!

% % Desired phase margin and conversion to radians
phase_margin = 55;
PM = phase_margin*pi/180;

% Phase of transfer function T1 at crossover frequency
% See figure 10-25.
fi_1 = phase(freqresp(T_converter, wcross))

% Calculate the needed phase-boost at the cross-over frequency
% See equation 10-112
boost = PM - fi_1 - pi/2;

% Calculate the factor K.
% See equation 10-108
K = tan(pi/4 + boost/2);
G=1/abs(freqresp(T_converter, wcross));
% Determine the component constants with help of the factor K.

```

```

% See equations 10-115, 10-115 and 10-117.
R1 = 2.43e3;
C2 = abs(freqresp(T_converter, wcross))/(K*wcross*R1);
C1 = C2*(K^2 - 1);
R2 = K/(C1*wcross);

% Integrator gain
% See equation 10-102
A = 1/(R1*C2);

% Controller zero
% See equation 10-104
wz = 1/(R2*C1); % -4.04e3;

% Controller pole
% See equation 10-105
wp = (C1 + C2)/(R2*C1*C2); % -4.1860e5;

% Transfer function for controller
% See equation 10-103
T_controller = A*((s + wz)/(s*(s + wp)));

%end
%

%% Including controller, PWM-modulator and power stage.
T_open_loop = T_controller*T_converter;

T_closed_loop = feedback(T_open_loop, 1);

% Make a step in the control voltage at t=0.8ms
[Y, X] = step(T_closed_loop, 2e-3);

figure;
plot(X*1e3, Y, 'b', 'LineWidth', 2);
%axis([0 0.5 4.8 6.5]);
xlabel('time [ms]');
ylabel('Output Voltage');
grid on
%%

```

```

disp('Design Parmeters of Compensation Network')

formatSpec = ('\nGain      : %.0f dB.\nZero      : %.0f rad/s.\nPole ...
: %.0f rad/s.\nR2      : %2.4f kOhm.\nC1      : %2.4fnF\nC2
...
: %2.4fnF\nRT1      : %2.4f kohm.\n\n');
fprintf(formatSpec,A,wz,wp,R2*1e-3,C2*1e9,C1*1e9,RT1)

formatSpec = ('Output1 Cap.      : %.0f uF.\nOutput2 Cap.
...
: %2.4f uF.\n\n');
fprintf(formatSpec,Co1*1e6,Co2*1e6)

```


B

Data sheets

B.1 N87 datasheet



Ferrites and accessories

SIFERRIT material N87

Date: September 2006

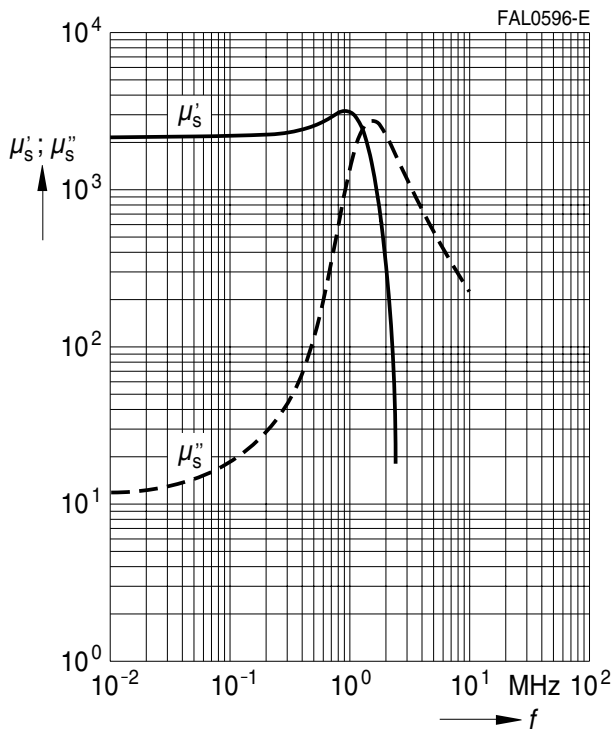
SIFERRIT materials
N87
Material properties

Preferred application			Power transformers
Material			N87
Base material			MnZn
	Symbol	Unit	
Initial permeability (T = 25 °C)	μ_i		2200 ±25%
Flux density (H = 1200 A/m, f = 10 kHz)	B _S (25 °C)	mT	490
	B _S (100 °C)	mT	390
Coercive field strength (f = 10 kHz)	H _c (25 °C)	A/m	21
	H _c (100 °C)		13
Optimum frequency range		kHz	25 ... 500
Hysteresis material constant	η_B	10 ⁻⁶ /mT	<1.0
Curie temperature	T _C	°C	>210
Mean value of α_F at 25 ... 55 °C		10 ⁻⁶ /K	4
Density (typical values)		kg/m ³	4850
Relative core losses (typical values)	P _V		
25 kHz, 200 mT, 100 °C		kW/m ³	57
100 kHz, 200 mT, 100 °C		kW/m ³	375
300 kHz, 100 mT, 100 °C		kW/m ³	390
500 kHz, 50 mT, 100 °C		kW/m ³	215
Resistivity	ρ	Ωm	10
Core shapes	RM, P, PM, ETD, EFD, E, ER, EP, EQ, ELP, U, Toroid		

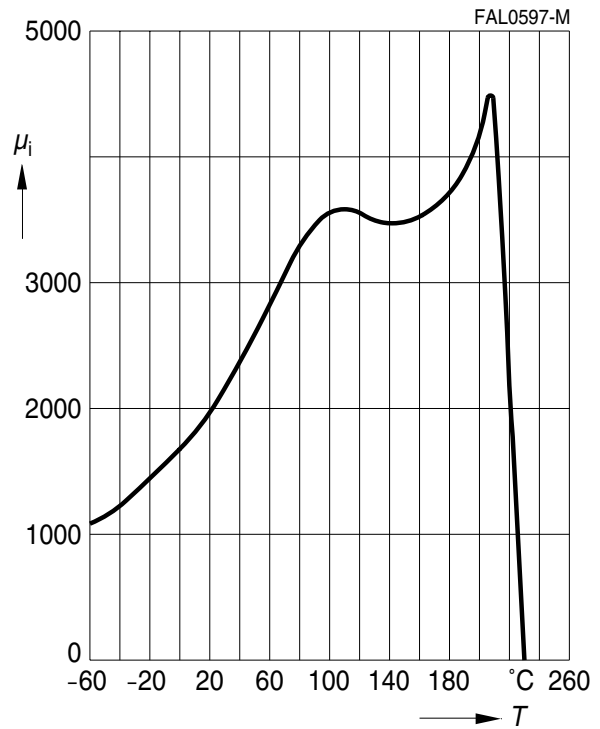
SIFERRIT materials

N87

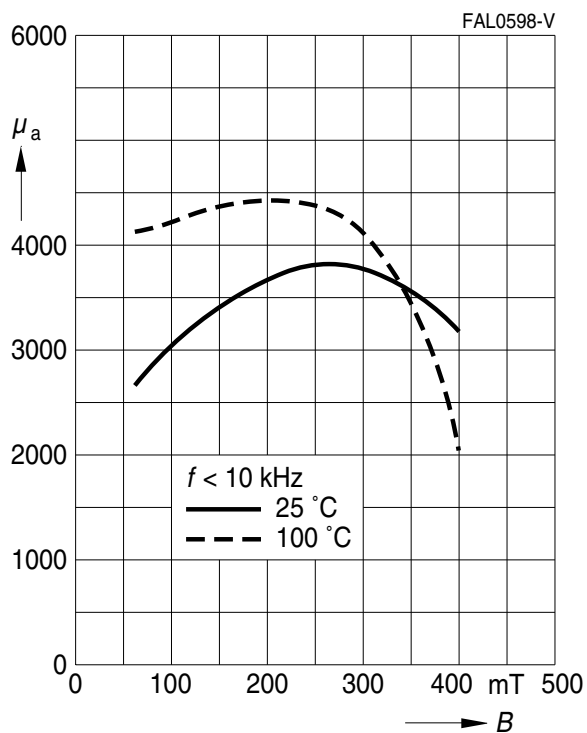
Complex permeability
versus frequency
(measured on R34 toroids, $\hat{B} \leq 0.25$ mT)



Initial permeability μ_i
versus temperature
(measured on R34 toroids, $\hat{B} \leq 0.25$ mT)



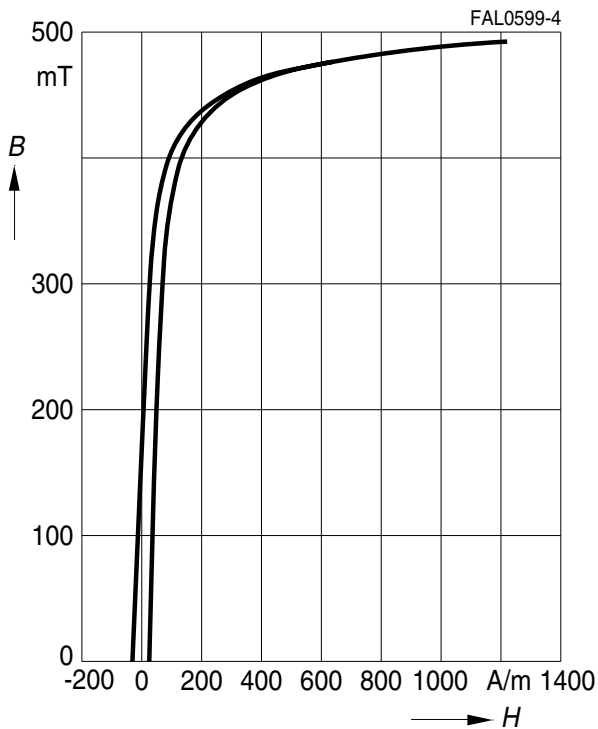
Amplitude permeability
versus AC field flux density
(measured on R34 toroids, $\hat{B} \leq 0.25$ mT)



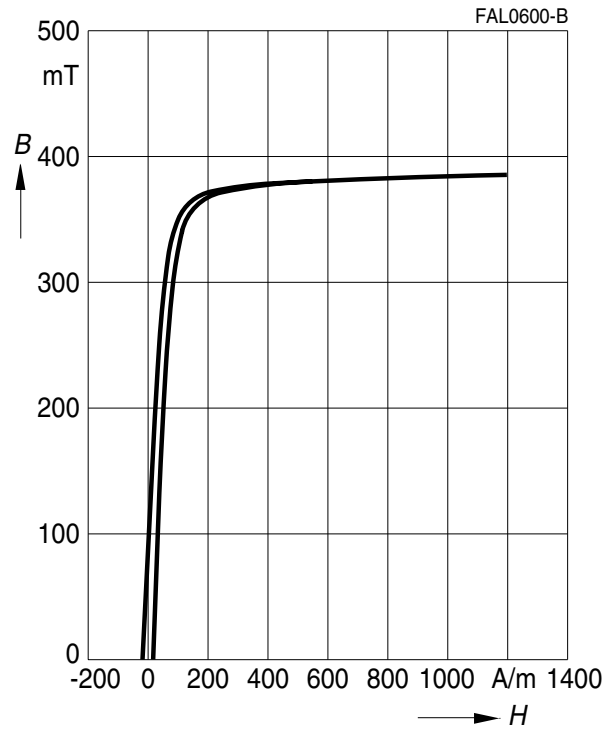
SIFERRIT materials

N87

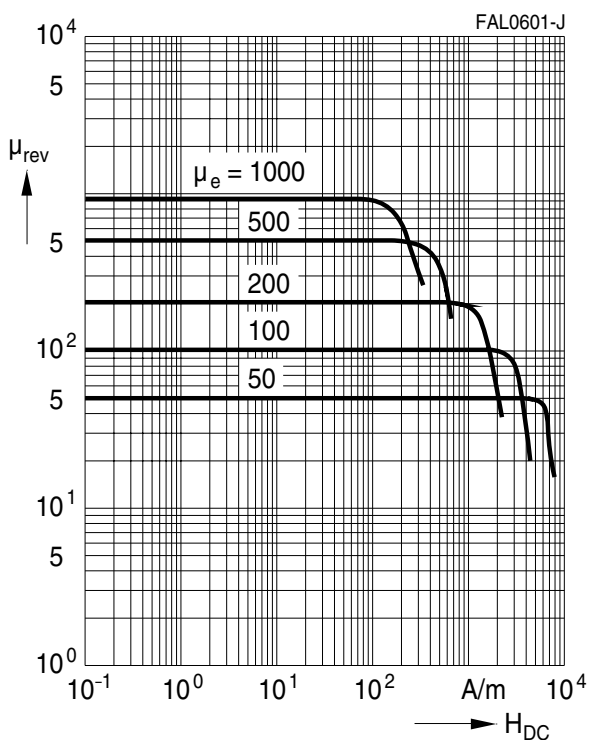
Dynamic magnetization curves
(typical values)
($f = 10 \text{ kHz}$, $T = 25 \text{ °C}$)



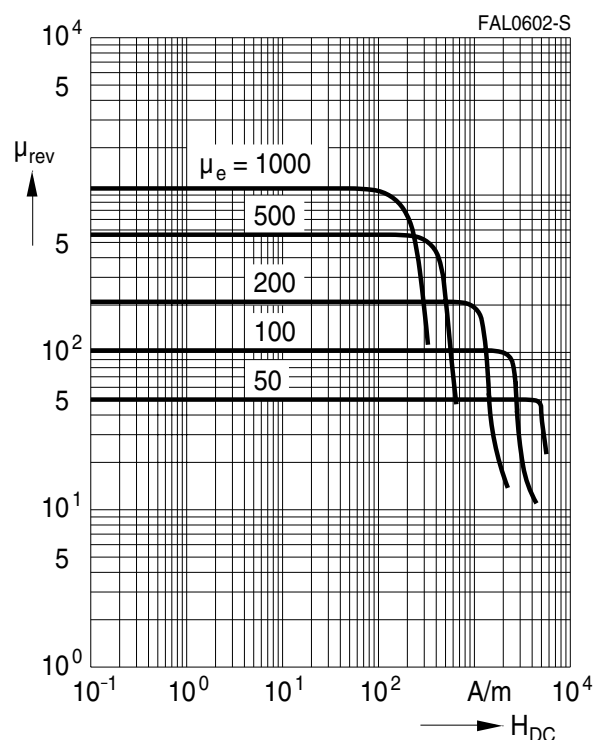
Dynamic magnetization curves
(typical values)
($f = 10 \text{ kHz}$, $T = 100 \text{ °C}$)



DC magnetic bias
of P, RM, PM and E cores
($\hat{B} \leq 0.25 \text{ mT}$, $f = 10 \text{ kHz}$, $T = 25 \text{ °C}$)



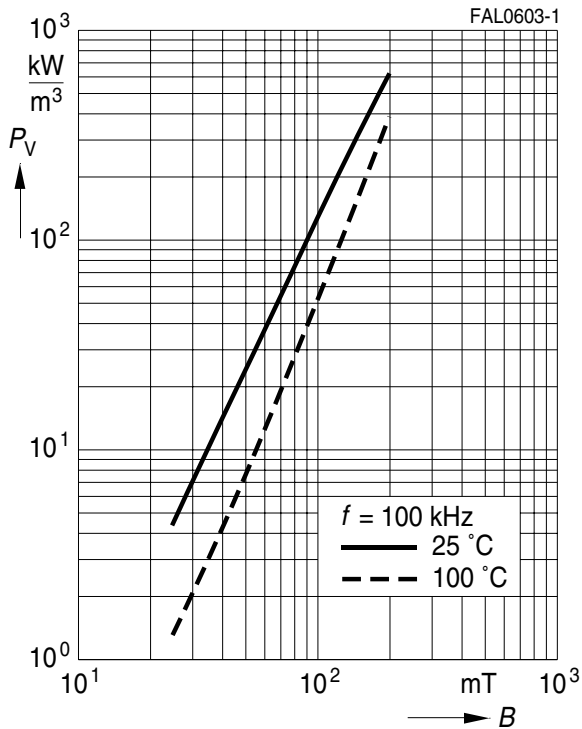
DC magnetic bias
of P, RM, PM and E cores
($\hat{B} \leq 0.25 \text{ mT}$, $f = 10 \text{ kHz}$, $T = 100 \text{ °C}$)



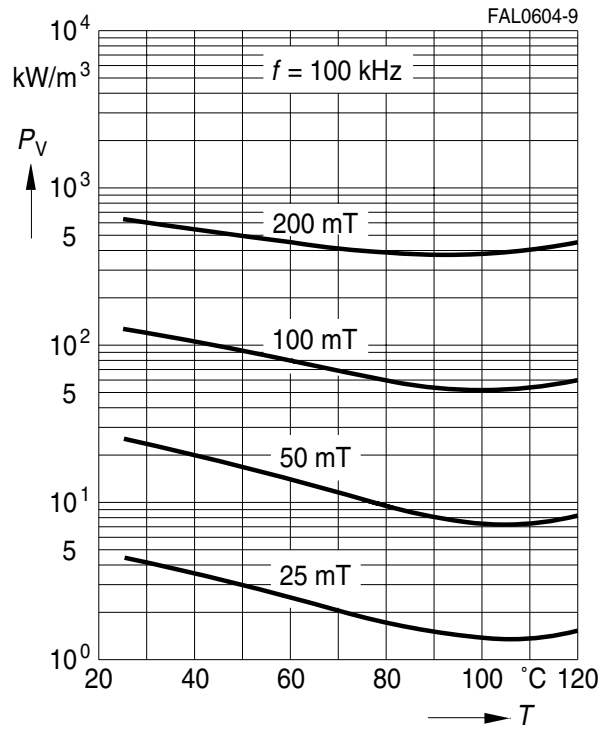
SIFERRIT materials

N87

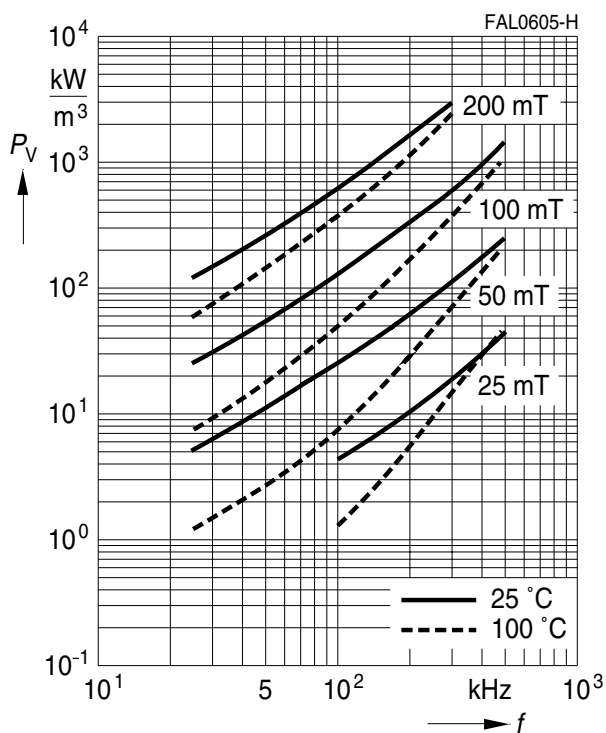
Relative core losses
versus AC field flux density
(measured on R34 toroids)



Relative core losses
versus temperature
(measured on R34 toroids)



Relative core losses
versus frequency
(measured on R34 toroids)



SIFERRIT materials**Cautions and warnings****General**

Based on IEC 60401-3, the data specified here are typical data for the material in question, which have been determined principally on the basis of toroids (ring cores).

The purpose of such characteristic material data is to provide the user with improved means for comparing different materials.

There is no direct relationship between characteristic material data and the data measured using other core shapes and/or core sizes made of the same material. In the absence of further agreements with the manufacturer, only those specifications given for the core shape and/or core size in question are binding.

Effects of core combination on A_L value

Stresses in the core affect not only the mechanical but also the magnetic properties. It is apparent that the initial permeability is dependent on the stress state of the core. The higher the stresses are in the core, the lower is the value for the initial permeability. Thus the embedding medium should have the greatest possible elasticity.

For detailed information see Data Book 2007, chapter "General – Definitions, 8.2".

Heating up

Ferrites can run hot during operation at higher flux densities and higher frequencies.

Important notes

The following applies to all products named in this publication:

1. Some parts of this publication contain **statements about the suitability of our products for certain areas of application**. These statements are based on our knowledge of typical requirements that are often placed on our products in the areas of application concerned. We nevertheless expressly point out **that such statements cannot be regarded as binding statements about the suitability of our products for a particular customer application**.

As a rule, EPCOS is either unfamiliar with individual customer applications or less familiar with them than the customers themselves. For these reasons, it is always ultimately incumbent on the customer to check and decide whether an EPCOS product with the properties described in the product specification is suitable for use in a particular customer application.

2. We also point out that **in individual cases, a malfunction of electronic components or failure before the end of their usual service life cannot be completely ruled out in the current state of the art, even if they are operated as specified**. In customer applications requiring a very high level of operational safety and especially in customer applications in which the malfunction or failure of an electronic component could endanger human life or health (e.g. in accident prevention or life-saving systems), it must therefore be ensured by means of suitable design of the customer application or other action taken by the customer (e.g. installation of protective circuitry or redundancy) that no injury or damage is sustained by third parties in the event of malfunction or failure of an electronic component.

3. **The warnings, cautions and product-specific notes must be observed.**

4. In order to satisfy certain technical requirements, **some of the products described in this publication may contain substances subject to restrictions in certain jurisdictions (e.g. because they are classed as hazardous)**. Useful information on this will be found in our Material Data Sheets on the Internet (www.epcos.com/material). Should you have any more detailed questions, please contact our sales offices.

5. We constantly strive to improve our products. Consequently, **the products described in this publication may change from time to time**. The same is true of the corresponding product specifications. Please check therefore to what extent product descriptions and specifications contained in this publication are still applicable before or when you place an order.

We also **reserve the right to discontinue production and delivery of products**. Consequently, we cannot guarantee that all products named in this publication will always be available.

The aforementioned does not apply in the case of individual agreements deviating from the foregoing for customer-specific products.

6. Unless otherwise agreed in individual contracts, **all orders are subject to the current version of the “General Terms of Delivery for Products and Services in the Electrical Industry” published by the German Electrical and Electronics Industry Association (ZVEI)**.

7. The trade names EPCOS, BAOKE, Alu-X, CeraDiode, CSMP, CSSP, CTVS, DSSP, MiniBlue, MKK, MLSC, MotorCap, PCC, PhaseCap, PhaseCube, PhaseMod, SIFERRIT, SIFI, SIKOREL, SilverCap, SIMDAD, SIMID, SineFormer, SIOV, SIP5D, SIP5K, ThermoFuse, WindCap are **trademarks registered or pending** in Europe and in other countries. Further information will be found on the Internet at www.epcos.com/trademarks.